FINAL REPORT FOR NASA GRANT NAGW-1646

Constraints on Cosmic Ray Propagation in the Galaxy

PI: James M. Cordes, Cornell University

In this project, we aimed at deriving a more detailed picture of MHD turbulence in the interstellar medium and its effects on cosmic ray propagation. To do so we have combined radio astronomical observations (scattering and Faraday rotation) with knowledge of solar system spacecraft observations of MHD turbulence, simulations of wave propagation, and modeling of the galactic distrubution to improve our knowledge. Scholarly products have included three Journal articles, contributions to two conference proceedings, and portions of a Ph.D. thesis at Cornell by Andrew Clegg, currently at the Naval Research Laboratory.

SUMMARY OF WORK DONE UNDER THE GRANT

During the grant period we have:

1. Developed a more sophisticated model for the galactic distribution of electron density turbulence. Through VLBI and pulsar observations of our own and others, we find that microturbulence in electron density (on scales of interest for cosmic ray propagation) is distributed according to two smooth components with embedded 'clumps' of especially strong turbulence. Our modeling has refined considerably the parameters of the two smoothly distributed components. An outer Galaxy component has a scale height of about 1 kpc and extends well beyond the solar circle at 8.5 kpc. The inner Galaxy component has a scale height of only 0.15 kpc and probably concides with the molecular ring seen from molecular line observations. Our modeling using an axisymmetric model for the distributions has been published recently in Nature, as cited below. As a follow-on to the grant-supported work, we are now extending the model to include spiral arms.
2. Analyzed Faraday rotation measure data to constrain magnetic field fluctuations in the ISM. The results are consistent with the notion that electron density fluctuations (which are easy to measure) are driven by magnetic field fluctuations, which are important for the energetics of the turbulence and for CR propagation.
3. Acquired VLBI observations of compact sources behind the supernova remnant CTA1. We expect that these observations will clearly determine whether the shock from this remnant is driving electron density variations. Our analysis of the VLBI data has proceeded slowly owing to problems with their calibration. However, we expect to obtain results of interest to the radio and cosmic-ray communities.
4. Made simple calculations about the energetics of the turbulence assuming a direct link between electron density and magnetic field variations. The energy contained in the turbulence is at least as large as what is in the large scale galactic field and is therefore important for the overall energetics of the ISM.
5. We have outlined a simulation of cosmic ray propagation through the Galaxy using the above results as input. The idea is to populate a pseudo Galaxy with magnetic field fluctuations that are consistent with the electron density model and an assumed relationship between density and magnetic field fluctuations (using Faraday rotation

studies and the CTA1 observations to calibrate the relation). The simulation output will be a pseudo cosmic ray energy spectrum as a function of line of sight, which we can compare with observed spectra and constraints on isotropy.

6. Used the above results combined with ideas about the origins of gamma-ray backgrounds from interactions of cosmic-rays with molecular line material as a basis for a proposal to the Gamma-ray Observatory Phase II. The idea is to use measurements of the γ-ray background to provide additional constraints on the spatial distribution of turbulence in the interstellar medium.
7. Run ray-tracing code through model shocks to determine what information may be extracted from 'extreme scattering events,' features in the intensity time series of extragalactic radio sources that seem to be due to relatively dense plasma clouds in the Galaxy. It appears that such clouds are over-pressured relative to the average pressure in the interstellar medium; therefore they must reside in regions of greater than average pressure such as is found in supernova shocks. This ray-tracing formed a chapter of Andrew Clegg's Ph.D. thesis.

PUBLICATIONS

1. 'Low Frequency Interstellar Scattering and Pulsar Observations' J. M. Cordes in **Low Frequency Astrophysics from Space**, eds. Kassim and Weiler, Lecture Notes in Physics 362, Springer-Verlag, 1990, pp. 165-174.
2. 'Fluctuations in the Galactic Magnetic Field' J. M. Cordes, A. W. Clegg, and J. H. Simonetti in **Galactic and Intergalactic Magnetic Fields**, IAU Proceedings, eds. Beck et al., pp. 55-58.
3. 'The Galactic Distribution of Free Electrons' J. M. Cordes, J. M. Weisberg, D. A. Frail, S. R. Spangler, and M. Ryan, **Nature**, 354, 121-124, 1991.
4. 'Interstellar Scattering towards the Galactic Center as Probed by OH/IR Stars', H. J. van der Langevelde, D. A. Frail, J. M. Cordes, and P. J. Diamond, **Astrophysical Journal**, in press, 1992.
5. 'Rotation Measures of Low Latitude Extragalactic Sources and the Magnetoionic Structure of the Galaxy' A. W. Clegg, J. M. Cordes, S. Kulkarni, and J. Simonetti, **Astrophysical Journal**, in press, 1992.
6. 'Radio Frequency Investigations of the Interstellar Medium' Ph.D. Thesis, Cornell University, 1991.

Interstellar scattering towards the Galactic center as probed by OH/IR stars.

Huib Jan van Langevelde *Sterrewacht Leiden, Leiden, the Netherlands*

Dale A. Frail *NRAO/AOC, Socorro, New Mexico, U.S.A.*

James M. Cordes *Astronomy department and N.A.I.C., Cornell University, Ithaca, New York, U.S.A.*

Philip J. Diamond *NRAO/AOC, Socorro, New Mexico, U.S.A.*

Summary. We report here on angular broadening measurements of 20 OH/IR stars near the Galactic center. This class of sources is known to have bright, intrinsically compact ($\leq$ 20 mas) maser components within their circumstellar shells. We have used VLBA antennas and the VLA to perform a MKII spectral line VLBI experiment. The rapid drop in correlated flux with increasing baseline, especially for sources closest to the Galactic center, is attributed to interstellar scattering. Angular diameters were measured for 13 of our sources. Lower limits were obtained for the remaining 7. With our data, together with additional data taken from the literature, we have been able to determine the distribution of interstellar scattering towards the Galactic center. We find a region of pronounced scattering ($\bar{\theta}_{obs}$ = 525 mas at 1.612 GHz) nearly centered (angularly) on SgrA*. We consider two interpretations for the enhanced scattering. One hypothesis is that the scattering is due to a clump of enhanced turbulence, such as those that lie along lines of sight to other known objects, that has no physical relationship to the Galactic Center. The other model considers the location of the enhanced scattering to arise in the galactic center itself. The physical implications of the models yield information on the nature of interstellar scattering. Future tests to discriminate between these models will be the measurement of angular sizes of extragalactic sources within 15′ of SgrA* and angular sizes of additional OH/IR stars toward the Galactic center region.

1. Introduction

It has long been suspected that the observed size of the Galactic center source SgrA* is set by interstellar scattering (Davies et al., 1976, Lo et al., 1981, Lo et al., 1985, Backer, 1988). At 1.6 GHz, the frequency we use throughout this paper, the scattered broadened diameter θ_{obs} of SgrA* is about 520 mas. Such a high value of interstellar scattering is unusual, as there are only a few lines of sight with comparable degrees of plasma turbulence (Cordes, Ananthakrishnan, and Dennison 1984; Moran et al., 1990, Fey et al., 1991). Is this scattering anomalous, local to SgrA* and a consequence of the activity occurring there (Backer, 1988)? Is it due to clumps of strong turbulence at some random position along the line of sight (Cordes, Weisberg, and Boriakoff, 1985)? Or can it be explained as part of the general increase in scattering that is observed towards the inner Galaxy (Fey et al., 1991, Rao & Slee, 1988)? The answer to this question has a bearing on an unsolved problem in the study of plasma turbulence in the interstellar medium: the identity of the agent(s) responsible for the turbulence.

Recently, van Langevelde & Diamond (1991) showed that the OH masers in the circumstellar shells of four OH/IR stars, all less than 16 arcmin from SgrA*, were broadened by an amount similar to SgrA*. Thus they confirmed that the size of SgrA* at centimeter wavelengths is set by interstellar scattering. An equally important consequence of this work was the realization that OH/IR stars are a powerful tool to study the turbulent electron density component in the very inner regions of our Galaxy. The number of observable OH/IR stars in this region is at least an order of magnitude larger than that of extragalactic sources, and they are all at roughly similar distances. Moreover, as we will show in section 2, there exist bright, intrinsically compact (< 20 mas) maser spots in all OH/IR stars and so the usual problem of intrinsic source structure for extragalactic sources does not enter into the interpretation of the visibility data. Pulsars, which in general are excellent point-source probes of interstellar scattering, cannot be used to obtain information on interstellar scattering close to the Galactic center. Although pulsars are probably present within a few kpc of the Galactic center (e.g. Clifton & Lyne 1986), it is unlikely that they will be found within 100 pc, because interstellar scattering will quench the pulsations.

In this paper we expand on the earlier work of van Langevelde & Diamond (1991) with the goal of determining the distribution of the scattering material around SgrA* in order to place constraints on the properties and the location of this medium. The outline of this paper is as follows. We start by describing our observational technique as it applies to the angular broadening of OH/IR stars specifically. This includes setting up the necessary formulas to describe scattering as well as the relation between interstellar scattering and the emission measure, which we will use to discuss the possibility of a scattering medium located at the Galactic center. In section 3 we discuss our source selection criteria, the observational parameters, and the reduction of the visibility data to scatter diameters. Finally, in section 4, we use these diameters, in addition to those from the literature, to examine possible models for the source of scattering in the direction of the Galactic center.

2. Technique

2.1. ANGULAR BROADENING BY INTERSTELLAR SCATTERING

Angular broadening has its origin in fluctuations of the electron density in the interstellar medium. Because the refraction index of the interstellar medium for radio waves is given by $n \approx 1 - (r_e n_e \lambda^2/2\pi)$, fluctuations in n_e cause disturbances in a wave front travelling through the interstellar medium. This degrades the degree of coherence between the signals received at two widely separated points, by an amount that depends on the level of turbulence present in the medium. Electron density fluctuations on scales of $10^6 - 10^8$ m are readily measurable with an interferometer by determining either the loss of coherence as a function of antenna separation (in the visibility plane) or, equivalently, the angular broadening (in the image plane).

The same fluctuations give rise to a variety of other observational phenomena (see Rickett, 1990, for a review), but we will concern ourselves in this paper with angular broadening alone. Following other authors in the study of the Galactic distribution of scattering material, we will make some simplifying assumptions. Apart from the fact that these assumptions are readily defendable, they also enable us to easily compare our results with others.

2.1.1. The power law description

Following Cordes, Weisberg and Boriakoff (1985), we describe fluctuations in the electron density by an isotropic power law:

$$P_{\delta n_e}(\mathbf{q}, x) = C_n^2(x) q^{-\alpha} \tag{1}$$

which holds between lower and upper wavenumber cutoffs: $q_0 \leq q \leq q_1$. $C_n^2(x)$ is the power in the fluctuation spectrum at some position along the line of sight (the changes in $C_n^2(x)$ take place on a much larger scale than the electron density fluctuations). There have been several studies specifically to determine α, q_0 and q_1 (Armstrong et al. 1981; Cordes et al. 1985, 1990; Gwinn et al. 1988; Spangler & Gwinn 1990). Determining these values is beyond the scope of our observations and so we use $\alpha = 11/3$ throughout this paper.

The power spectrum above will produce a phase structure term in a propagating wave through the medium. This will affect the measured visibility of a point source at a distance L, which is described by,

$$V(\rho, L) = \exp[-D_\phi(\rho)/2] \tag{2}$$

where ρ is the baseline length and $D_\phi(\rho)$, the phase structure function, is given by

$$D_\phi(\rho) = 8\pi^2 r_e^2 \lambda^2 \int_0^L \int q[1 - J_0(q\rho)] P_{\delta n_e}(q, x) dq\, dx$$

for the case of a plane wave (source at infinity). For a source embedded in the medium, it has been shown (Ishimaru, 1978, p. 418) that $J_0(q\rho)$ is replaced by $J_0(q\rho x/L)$ where (x/L) is a dilution factor. For $2\pi/q_1 \ll \rho \ll 2\pi/q_0$, this results in,

$$V(\rho, L) = \exp[-(\rho/\rho_c)^{\alpha-2}] \tag{3}$$

where

$$\rho_c = [4\pi^2 \lambda^2 r_e^2 S(L) f(\alpha)]^{-1/(\alpha-2)} \tag{4}$$

in which $f(\alpha)$ is an integration constant equal to 1.11835 for $\alpha = 11/3$. $S(L)$ takes into account the integration of $C_n^2(x)$ from source to observer. It equals

$$S(L) = \int_0^L C_n^2(x)(\frac{x}{L})^{\alpha-2} dx \tag{5}$$

when the observed source lies within the medium, or

$$S(L) = \int_0^L C_n^2(x) dx \tag{6}$$

when observing an extragalactic source. In this last case $S(L)$ is by definition the scattering measure, SM. This quantity is directly usable in the case of an extragalactic source. For a source embedded in the medium, as in this work, an additional assumption is needed before the SM can be used. If we make $C_n^2(x)$ constant, equation (5) can be expressed as $S(L) = (\alpha - 1)^{-1} SM$ (Cordes et al., 1991a). If C_n^2 is not a constant then equation (5) should be used. Note that there is a strong weighting of scattering along the line of sight. The effect is that electron turbulence close to the source is weighted much less strongly [$\propto (x/L)^{\alpha-2}$] than material more distant from the source.

2.1.2. The very strong scattering regime

The analysis embodied in equations (3) to (5) assumes that the relevant baselines (i.e. $\rho \approx \rho_c$) are bracketed by the inner and outer scales of the electron density power spectrum:

$$\ell_1 \equiv 2\pi q_1^{-1} \ll \rho \ll \ell_0 \equiv 2\pi q_0^{-1}. \tag{7}$$

In very strong scattering, the visibility function becomes narrower than the inner scale, ℓ_1. In this case, different expressions for the scattering measure hold. Other researchers (e.g. Spangler and Gwinn 1990; Moran et al. 1990; Molnar et al. 1990) have found evidence in favor of an inner scale $\ell_1 \approx 100$ km, suggesting that any measured angular diameters θ_{obs} smaller than about 100 mas at 1 GHz are influenced by finite inner scale effects.

There are several consequences of a finite inner scale which should be mentioned. First, very strong scattering that yields a very small spatial scale for the visibility *does not* require correspondingly small scale sizes in the scattering medium. Second, in very strong scattering, the visibility function is a Gaussian and the scattering diameter scales as $\theta_{obs} \propto \lambda^2$. Thus

$$V(\rho, L) = \exp[-(\rho/\rho_c)^2] \tag{8}$$

where it can be shown (e.g. Cordes and Lazio 1991) that

$$\rho_c = \left[2\pi^2 \lambda^2 r_e^2 S(L)\, q_1^{4-\alpha} (4-\alpha)^{-1}\right]^{-1/2}. \tag{9}$$

Third, the line-of-sight weighting is changed slightly, such that, for sources embedded in the medium, equation (5) is replaced with

$$S(L) = \int_0^L C_n^2(x)(\frac{x}{L})^2 dx \ . \tag{10}$$

The result of equation (6) still holds for extragalactic sources.

2.1.3. *Resulting expressions*

In general we give the following result, expressed in observable quantities

$$S(L) = \begin{cases} \left(\frac{\theta_{obs}}{133\,\mathrm{mas}}\right)^2 \left(\frac{\ell_1}{100\,\mathrm{km}}\right)^{1/3} \nu_{\mathrm{GHz}}^4 & \theta_{obs} \geq \theta_{cross} \\ \left(\frac{\theta_{obs}}{128\,\mathrm{mas}}\right)^{5/3} \nu_{\mathrm{GHz}}^{11/3} & \theta_{obs} \leq \theta_{cross} \end{cases} \quad (11)$$

where $\theta_{cross} \approx 0.16''(\nu_{\mathrm{GHz}}(\ell_1/100\ \mathrm{km}))^{-1}$.

To give the reader some idea about the numbers involved, we mention here that the values of $C_n^2(x)$ determined for the solar neighborhood are $\sim 10^{-3.5}\mathrm{m}^{-20/3}$, resulting in an angular size of about 1 mas for an extragalactic source at 18 cm for a line of sight of 1 kpc through the medium. C_n^2 is typically 1 $\mathrm{m}^{-20/3}$ in the inner Galaxy, resulting in up to 150 mas for objects seen *through* the inner Galaxy.

2.1.4. *Electron Densities and Emission Measures*

The electron density variations responsible for scattering also contribute to free-free radiation. The calculation of the emission measure EM involves $n_e = \overline{n}_e + \delta n_e$ with $\overline{n}_e$ the local mean density and δn_e the local variation about the mean. To estimate the rms electron density δn_e one integrates $P_{\delta n_e}$, the fluctuation spectrum. For $\alpha = 11/3$ and an outer scale $\ell_0 \gg \ell_1$,

$$\delta n_e(rms) = (6\pi C_n^2)^{1/2} \left(\frac{l_0}{2\pi}\right)^{1/3} \approx 0.03\ \mathrm{cm}^{-3} \left(\frac{C_n^2}{10^{-3}\,\mathrm{m}^{-20/3}}\right)^{1/2} \left(\frac{\ell_0}{1\ \mathrm{pc}}\right)^{1/3}. \quad (12)$$

This will give a contribution to the EM, which may be written as

$$EM_{\mathrm{SM}} \approx \frac{2(2\pi)^{4-\alpha}}{\alpha - 3} \ell_0^{\alpha-3} SM = 10^{2.74}\,\mathrm{pc\ cm}^{-6} \left(\frac{\ell_0}{1\ \mathrm{pc}}\right)^{2/3} \left(\frac{SM}{1\ \mathrm{kpc\ m}^{-20/3}}\right) \quad (13)$$

(Cordes et al. 1991a,b). This corresponds to a minimum optical depth

$$\tau_{ff,\mathrm{SM}} = \frac{1}{10^{3.54}} \left(\frac{SM}{1\ \mathrm{kpc\ m}^{-20/3}}\right) \left(\frac{\ell_0}{1\ \mathrm{pc}}\right)^{2/3} \frac{g(\nu, T)}{\nu_{\mathrm{GHz}}^2\, T_4^{1.5}} \quad (14)$$

where $T_4 = (T/10^4\,K)$ and $g(\nu, T) = 1 + 0.085 \ln T_4 + 0.387 \ln \nu_{\mathrm{GHz}}$. Density fluctuations are bounded, locally, by $\delta n_e \leq \overline{n}_e$, so the actual EM and optical depth are *at least* a factor of two larger than the values in equation (13) and equation (14).

2.2. OH/IR STARS

In order to fully appreciate why we can use OH/IR stars to study interstellar scattering, we must first discuss the properties of OH masers in circumstellar shells. From the moment of their discovery it was suggested that the strong 1612 MHz spectral lines with their typical two-peaked signature are caused by maser emission in *expanding* circumstellar shells (Wilson & Barett, 1968). In the last two decades several aspects of these OH/IR stars have become clear. First, we now know that the underlying stars are objects on the Asymptotic Giant Branch. Having reached their final stages of evolution, these stars are losing a considerable percentage of their mass ($\leq 10^{-4}\,\mathrm{M}_\odot/\mathrm{yr}$),

resulting in a circumstellar shell which is gradually flowing away from the star. Dust condenses in this shell and is responsible for the prominent IR signature of these stars. Because of the large, cool, optically thick dust shell we see all the luminosity of the giant star being emitted longward of $5\mu m$.

This IR emission causes a population inversion in the OH molecules, which are abundant in the shell. Provided that long coherent pathlengths are available, line emission in such a medium can develop into a maser. Precisely because the shell is expanding, the maser works most efficiently along the radial lines in the shell. Here all OH molecules in the shell can "see" one another; in more tangential lines the different parts of the shell cannot amplify each other's emission because of a relative Doppler shift. Therefore every observer in any direction from the star sees the brightest emission from the extreme back and front of the shell, the outermost blue- and redshifted parts of the spectrum.

This maser beaming, arising from the fact that the shell is expanding, results in a higher brightness temperature for the peaks of the spectrum than for the inner parts.

From interferometric observations it is clear that the brightness temperatures of the inner parts of the spectrum are typically of the order of 10^4 K, while for the peaks of the spectrum this can be at least 10^8 K (see Alcock & Ross, 1988, and references therein). In several cases (Norris et al., 1984, Benson & Mutel, 1979, Bowers et al., 1980, Reid et al., 1977) hotspots with angular sizes of the order of 10 mas are detected which have corresponding 10^9- 10^{10} K brightness temperatures.

2.3. OH/IR STARS AS PROBES OF INTERSTELLAR SCATTERING

In this paper we interpret measurements of the angular sizes of the peak maser emission from OH/IR stars as scatter broadening caused by interstellar scattering. Of course we can do this only when we can safely rule out that the intrinsic angular brightness distribution has no effect on our measurements, treating the underlying OH masers as point sources. For most sources in the survey we present here, we detect brightness temperatures of just 10^6 K for the peak of the spectrum, which we safely attribute to interstellar scattering. In this respect it is interesting to discuss the result by Diamond et al. (1988), who show that the angular sizes of the peaks in OH/IR stars increase with distance. This result indicates that interstellar scattering determines the sizes (and brightness temperatures) for OH masers at large distances, as had been suspected earlier (Burke et al., 1968, Boyd & Werner, 1972, Moran et al., 1973, Bowers et al., 1980, Kent & Mutel, 1982, Gwinn et al., 1988, Kemball et al., 1988).

Because all these authors fail to find sources with angular sizes less than 20 mas more distant than 1 kpc, there is good reason to believe that the maximum brightness temperature measurements for OH masers are frequently limited by interstellar scattering. With this in mind, we feel safe to use all measurements of the angular size above 50 mas as a measurement of interstellar scattering for sources at the distance to the Galactic center. This might also be valid for sources with smaller sizes, but to be conservative these should be interpreted as upper limits on angular broadening.

TABLE 1
LIST OF OBSERVED OH/IR STARS

Source Name	RA (1950)	DEC (1950)	Peak Velocities ($km\ s^{-1}$)		Peak Fluxes (Jy)		IRAS Designation
(1)	(2)	(3)	(4)		(5)		(6)
OH 357.849+9.744	17 00 49.34	−25 12 23.3	−31.6	−11.2	1.7	0.5	17008−2512
OH 0.125+5.111	17 23 22.90	−26 02 24.1	−151.4	−135.6	2.3	1.1	17233−2602
OH 353.298−1.537	17 31 36.51	−35 23 55.9	48.5	74.6	3.1	3.6	17316−3523
OH 359.140+1.137	17 35 56.95	−29 02 24.7	−145.7	−127.5	2.4	1.8	17359−2902
OH 359.564+1.287	17 36 24.70	−28 36 10.0	17.9	45.2	1.7	0.5	17364−2836[a]
OH 355.641−1.742	17 38 34.34	−33 32 13.9	−245.7	−224.2	3.3	5.1	17385−3332
OH 355.897−1.754	17 39 16.11	−33 19 36.1	−58.0	−30.8	1.1	1.4	17392−3319
OH 0.892+1.342	17 39 24.74	−27 27 02.0	−123.3	−93.7	49	0.8	17393−2727
OH 1.212+1.258	17 40 29.90	−27 13 25.3	30.4	57.7	5.8	4.9	17404−2713
OH 359.517+0.001	17 41 16.555	−29 19 35.19	−145.6	−111.5	0.9	1.5	
OH 359.762+0.120	17 41 24.132	−29 03 20.94	−21.0	9.6	1.8	3.3	
OH 1.369+1.003	17 41 50.64	−27 13 30.4	−27.4	3.3	8.7	6.8	17418−2713
OH 359.581−0.240	17 42 22.155	−29 23 56.71	−103.6	−75.2	3.1	0.9	
OH 359.880−0.087	17 42 29.643	−29 03 53.70	−34.6	−14.2	6.6	2.0	
OH 359.986−0.061	17 42 38.757	−28 57 40.35	−7.4	50.5	1.2	1.0	
OH 0.319−0.040	17 43 21.902	−28 39 58.32	57.3	92.2	1.3	3.4	
OH 0.814+0.179	17 43 41.639	−28 07 47.81	56.2	88.8	0.5	1.9	
OH 0.334−0.181	17 43 56.62	−28 43 39.1	−356.4	−326.9	3.5	2.9	
OH 5.026+1.491	17 48 26.09	−23 50 56.3	106.7	135.1	3.0	1.2	17484−2350[b]
OH 3.234−2.404	17 59 18.87	−27 21 58.8	−45.2	−20.2	4.6	0.2	17593−2721[c]

a. 17363−2833 *b.* 17486−2345 *c.* 17596−2716

3. Observations

3.1 SOURCE SELECTION

In order to map the distribution of interstellar scattering about SgrA*, we require a large sample of bright OH/IR stars. Fortunately, there is a strong concentration of OH/IR stars within one degree of the Galactic center (Lindqvist et al., 1991). Approximately half of the 20 OH/IR stars used in our work (see table 1) were taken from the Lindqvist et al. (1991) survey in which 134 sources were discovered in the central 1.5 square degrees of our Galaxy. Since the VLA [1] was used for their survey, subarcsecond positions were already available for our work. For sources that have $|b| > 0.5°$, the all-sky survey of te Lintel Hekkert et al. (1991) was used instead. The best positional information in the te Lintel Hekkert et al. (1991) survey was based upon a match between the OH/IR star (detected at 1612 MHz) and its nearest IRAS point source with the proper colors. These positions were only accurate to ±15 arcsec and so a short VLA astrometry program had to be carried out before the VLBI observations could be done.

[1] The Very Large Array (VLA) and the Very Long Baseline Array (VLBA) are operated by the National Radio Astronomy Observatory under cooperative agreement with the National Science Foundation.

3.2. ASTROMETRY

On June 21, 1990 the VLA was used in the hybrid A/B array configuration and two polarizations of 64 spectral line channels each were recorded across a bandwidth of 391 kHz (or 6.1 kHz per channel). The data were reduced within the AIPS package following standard practice. Table 1 contains the results of this work along with the positions of the lower latitude sources from the Lindqvist et al. (1991) catalog. Column (1) lists the source name given with a preface of "OH", followed by its galactic coordinates, while columns (2) and (3) are the right ascension and declination of each source, respectively. Column (4) gives the velocities for the blue- and red-shifted peaks of the double-peaked profiles. Similarly, the peak flux densities for these components are given in column (5). Because OH/IR stars are known to be highly variable these values should only be taken as approximate.

We observed 15 OH/IR stars from the catalog by te Lintel Hekkert et al. (1991); 13 were detected. 17338−2744 and 17392−2722 were not detected. For all but one of the 13 detected sources there is an IRAS source name in column (6). OH 0.334−0.181 was paired with 17439−2845 by te Lintel Hekkert et al. (1991), but at our new VLA position, 1.5 arcminutes away, there is no known IRAS source. This is likely due to confusion in the IRAS data, because of the low latitude. Another 3 OH/IR stars out of these 13 were found to be associated with an IRAS point source other than the one that te Lintel Hekkert et al. (1991) assigned. The original IRAS names of these sources are found just below Table 1. Apart from these 6 cases we believe the other IRAS assignments to be correct. The poor detection statistics should not be taken as typical for the te Lintel Hekkert et al. (1991) survey, because the stellar density is very high in this region. There are no IRAS designations for the Lindqvist et al. (1991) sources in table 1, owing to the severe confusion that occurs in the infrared at these lower latitudes.

3.3. THE DISTANCE PROBLEM

The selection of appropriate OH/IR stars from these catalogs was governed primarily by considerations of sensitivity. In order to make a detection within the coherence time on a VLA-VLBA baseline with the characteristically small linewidths of these masers ($\sim$ 6 kHz), we must select stars with a peak flux above 1.5 Jy. This condition was relaxed somewhat in a few instances along interesting lines of sight. In addition, as a check, we included one of the sources from van Langevelde & Diamond (1991).

To simplify any comparison of the scattering properties between these different lines of sight, it is important to choose the sample of OH/IR stars so that they are located at or beyond the Galactic center. From their flattened distribution and kinematics we know, at least in a statistical sense, that the Lindqvist et al. (1991) survey contains stars at the Galactic center. For the te Lintel Hekkert et al. (1991) sample, the situation is a bit less certain because the density contrast towards the center θ_{obs} of the Galaxy is less pronounced than in the Lindqvist et al. (1991) sample. Fortunately, the IRAS data yield a useful discriminant. While the 1612 MHz maser emission can vary widely from one star to the next (Gaylard et al., 1989, Röttgering, 1989, Dickinson, 1987), the variation in bolometric stellar luminosity is relatively more well-behaved. This enables us to obtain some distance information about individual objects.

Thus, obvious foreground stars can be eliminated from our sample by choosing only those stars whose IRAS fluxes are weak. We have estimated a distance from the IRAS

12 and 25 μm bands using a standard luminosity of 15000 $L_\odot$, which is a reasonable estimate of the luminosity of these OH emitting AGB stars (*e.g.* van Langevelde et al, 1990). For this estimate we have used the bolometric correction for OH/IR stars given by van der Veen & Breukers (1989). We eliminated all sources whose distances calculated in this manner were less than 8 kpc. Work to derive the IR fluxes for the low latitude sources in Lindqvist et al. (1991) is in progress (Blommaert, private communication).

3.4. VLBI OBSERVATIONS

The observations were made on two separate occasions, October 18, 1990 and February 1, 1991. The phased VLA and all the working antennas of the VLBA were used in both cases. This included antennas at Pie Town (PT), Los Alamos (LA), Kitt Peak (KP), and Fort Davis (FD). The point source calibrator 1748−253 was observed for several minutes each half hour to re-phase the elements of the VLA, and the bright source NRAO 530 was observed every 4 hours to act as a "fringe finder" during correlation. Each OH/IR star was observed for 10-12 minutes at a time, with two scans made at different hour angles so as to sample a full range of baseline lengths.

The data were recorded on MkII tapes with a total bandwidth of 500 kHz. The tapes were processed on the NRAO MkII correlator, splitting the bandwidth into 96 spectral line channels of 5.2 kHz each (0.97 km s^{-1}). After correlation the data were further processed in AIPS following procedures outlined by Diamond (1989). The bandpass correction was made using the total power spectrum from each antenna for NRAO 530 and the data were corrected for Doppler tracking. In the first session, the amplitude calibration was done in the same manner as explained in van Langevelde & Diamond (1991) by using the monitored system temperatures and estimated antenna gain factors, in much the same way as is done with continuum VLBI. In the second session, however, the VLA data showed signs of severe broadband contamination, most likely from the GLONASS network of satellites. A full amplitude calibration was impossible. Instead we either estimated calibration constants from *a priori* information, or used only VLA-VLBA baselines for further analysis. Because all VLBA antennas are essentially identical, we expected VLA-VLBA baselines to be equally sensitive within 10%, as was found during the first run.

A fringe fit was done for our calibrator, NRAO 530. We also had observations of 1748−253 every half hour to re-phase the VLA, so we were able to use it to fringe fit. In this way we obtained reasonable solutions for delay and fringe rates for all antennas during the *entire* observation period. We then continued with a fit of the residual fringe rate on the OH maser sources, setting a window on the spectral channels in which we expected the peak fluxes. We set the threshold for an acceptable detection to 4σ, where we had limited the search for a fringe to the spectral channel where we expected a signal. By performing a residual fringe fit we gave up the absolute position information on the OH source.

In principle, the final step in obtaining the results we are interested in is straightforward. We have the spectrum of the source from a number of baselines and a "zero spacing" measurement from the autocorrelation spectrum on any of the telescopes. The autocorrelation spectrum on the VLA is most often used for the latter, because it has the highest signal-to-noise and benefits from the lower confusion provided by its small synthesized beam. At this point we simply fit a Gaussian profile to the visibility

data of the brightest channel. We determine θ_{obs}, the full width at half maximum of the corresponding Gaussian in the map plane, directly from this value.

Our basic dataset and fitting procedure is illustrated in figure 1 where we show the results for OH 0.125+5.111. Although this is a relatively weak source, it was detected on all the baselines present (PT-LA is missing, because of a technical problem). Note that this particular source is not heavily scattered, while for most of the sources in our sample, detections were made on only the shortest and most sensitive baselines.

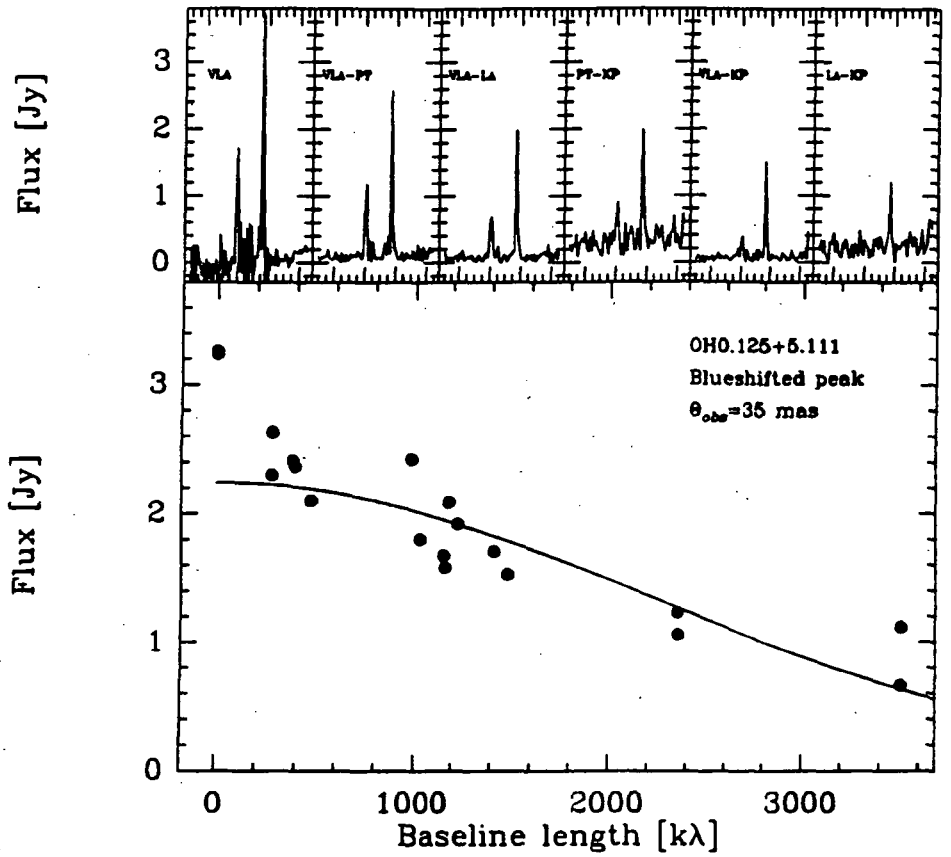

Figure 1. The amplitude of OH 0.125+5.111 as a function of baseline. The top row shows the spectra as detected on baselines of increasing length towards the right. The bottom shows the amplitude of the brightest, blue-shifted peak as a function of baseline length together with the fitted model for a spherical gaussian. Because we assume a single component and the data have been subjected to fringe fitting we disregard the phase information and take it to be zero on average.

In table 2 we list the measured angular sizes θ_{obs} of all sources which were detected on one or more baselines. Also given in table 2 is the log of the scattering measure for a scattering medium assumed to have constant $C_n^2(x)$. The last column in table 2 is the angular distance from SgrA*. Seven of our 20 sources were not detected on any of the measured baselines but were seen in the autocorrelation spectra. For three of these sources we did not have data for our shortest baselines, because of a failure at PT, so it is perhaps not surprising that we did not detect these.

We do not give errors on the measurements for each source in table 2. An accurate estimate of the uncertainties in the angular sizes is difficult to give, especially for the

larger scattering sizes. They can generally not be estimated from the formal errors in the fit because the large angular sizes are often based on detections of a single baseline and are therefore a strong function of calibration and the detection threshold. Taking this into consideration we estimate the errors on the large scatter sizes to be as high as 30%. For the small scatter sizes we think we can rely upon the formal errors in the fit being on the order of 5% - 10%.

TABLE 2
SCATTERING DIAMETER MEASUREMENTS
OF OH/IR STARS AT 1612 MHz

Source Name (1)	θ_{obs} (mas) (2)	log SM† (kpc $m^{-20/3}$) (3)	ΔSgrA* (arcmin) (4)
OH 353.298−1.537	360	2.17	408.6
OH 355.641−1.742	329	2.09	277.5
OH 355.897−1.754	348	2.14	263.5
OH 357.849+9.744	157	1.45	600.6
OH 359.140+1.137	269	1.92	85.8
OH 359.564+1.287	81	0.86	83.2
OH 359.762+0.120	495	2.45	14.8
OH 0.125+5.111	35	0.25	309.6
OH 0.892+1.342	57	0.60	100.9
OH 1.212+1.258	258	1.88	109.1
OH 1.369+1.003	112	1.16	106.2
OH 3.234−2.404	141	1.36	242.8
OH 5.026+1.491	68	0.73	318.5

† Assuming a medium with uniform C_n^2 and ℓ_1 = 100 km.

3.5. KNOWN LINES OF SIGHT

To aid in our discussion we can enlarge the number of sampled lines of sight by including measured angular diameters from the literature. The 4 OH/IR stars of van Langevelde & Diamond (1991) were taken from the Lindqvist et al. (1991) sample and were observed with exactly the same telescope array and procedures as described above. We also use the measurements of OH and H_2O masers in the SgrB2 complex (Gwinn et al. 1988, Moran, 1968). In addition, two radio transients have been discovered close to the Galactic center, both of which have had angular broadening measurements made over a range of wavelengths (Zhao et al. 1991, Davies et al. 1976). Finally, of course, we include SgrA* itself (Lo et al., 1985). For these last four sources it is known that their angular sizes scale quadratically with wavelength, consistent with their sizes being determined by interstellar scattering. The authors in each of the above-mentioned references also argue that their sources are located at the Galactic center. These extra eight lines of sight are presented in table 3 in much the same format as table 2.

TABLE 3
ADDITIONAL ANGULAR BROADENING MEASUREMENTS SCALED TO 1612 MHz

Source Name (1)	l (degrees) (2)	b (degress) (3)	θ_{obs} (mas) (4)	log SM (kpc m$^{-20/3}$) (5)	ΔSgrA* (arcmin) (6)	Ref. (7)
OH 359.762+0.120	359.762	0.120	531	2.51	14.8	1
OH 359.938−0.077	359.938	−0.077	571	2.57	1.9	1
GCT	359.939	−0.055	500	2.46	0.6	2
SgrA*	359.944	−0.046	520	2.49	0.0	3
A 1742−28	359.930	−0.043	530	2.51	0.9	4
OH 359.954−0.041	359.954	−0.041	591	2.60	0.7	1
OH 0.190+0.036	0.190	0.036	103	1.08	15.6	1
SgrB2	0.7	0.01	96	0.98	45.5	5

(1) van Langevelde and Diamond (1991) (2) Zhao *et al.* (1991) (3) Lo *et al.* (1985) (4) Davies *et al.* (1978) (5) Moran (1968).

4. Discussion

OH 359.762+0.120 was observed both here and by van Langevelde & Diamond (1991), and the θ_{obs} agree within the errors.

Figure 2 shows the distribution of scattering sizes in galactic coordinates for the data taken from Tables 2 and 3. The sizes of the open circles are directly proportional to θ_{obs}. The most striking aspect of this figure is the concentration of large scattering sizes near SgrA*. This is more evident in Figure 3 where we show the observed scatter size as a function of distance from SgrA*. There are 7 measurements within $\pm$15 arcmin of SgrA* with an average θ_{obs} of 525 mas. In addition, we draw attention to the lower limits on θ_{obs} (upper limits on correlated flux) found on the left hand side of figure 3. These are the 7 sources for which we failed to detect VLBI fringes. They are not randomly distributed about the range of sampled distances from SgrA*, as would be expected if our non-detections were due to errors in pointing or poor sensitivity. It suggests that these lines of sight are more scattered still and that they are all but resolved by even our shortest baselines.

There are prominent variations in θ_{obs} in figure 2 over short angular scales. Beyond the central region of 15 arcmin radius, θ_{obs} drops precipitously to a value of 100 mas. Two sources are responsible for the drop, SgrB2 and OH 0.190+0.036. In the past this result for SgrB2 has been used to define the outer limit for the size of the scattering region around SgrA* to be 45 arcmin, or a maximum length scale of 150 pc (Backer, 1978, Ozernoi & Shishov, 1977). With OH 0.190+0.036 we can constrain the outer extent further still to 15 arcmin, or a radius of 40 pc. However, we caution that there are no IRAS colors for this star; thus the possibility exists that it is a foreground object. At $b \sim 1.5$ degrees there are two additional examples of prominent variations taking place on short angular scales. Two pairs of sources, OH 359.140+1.137 and OH 359.564+1.287, and OH 1.212+1.258 and OH 0.892+1.342, are believed to be located at or beyond the galactic center on the basis of their IRAS fluxes. In each pair the ratio of θ_{obs} varies by a factor of 3-5 over angular scales of 20-25 arcmin, which corresponds to order-of-magnitude variations in SM, over a maximum transverse distance of only 50-65 pc (but an unknown distance along the line of sight). We also note that the data do not prove that scattering decreases monotonically from the Galactic center, because some of the lower bounds are more than a factor of two larger than actual detections for similar angular distances from the Galactic center.

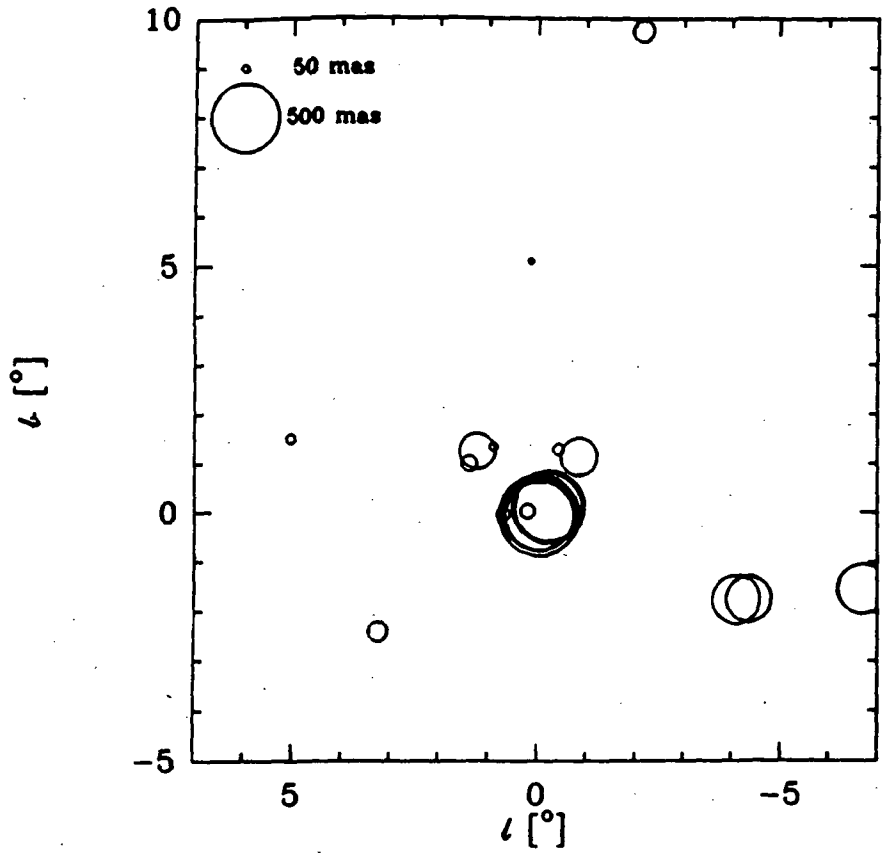

Figure 2. Scattering sizes for all the lines of sight near the Galactic center. The sizes of the circles indicate the amount of observed angular broadening.

4.1. COMPARISON WITH OTHER SCATTERING MEASUREMENTS

To put the Galactic center source measurements into context, we show in Figure 4 their scattering measures along with those of pulsars, other maser sources, and one active galactic nucleus (this figure is copied from Cordes et al. 1991a) for the area $-30° < l < 30°, -10° < b < 10°$. As can be seen, SM increases with distance much faster than would be expected if C_n^2 were constant and equal to the value inferred for the local interstellar medium. The rise occurs within the first few kpc from the Sun. The solid line in Figure 4 displays SM predicted from a best fit model (Cordes et al. 1991a) to more than 200 lines of sight. The model consists of an outer Galaxy component that is nearly constant in galactocentric radius and has a z scale height of 1 kpc; an inner Galaxy annulus is centered on $R \approx 4$ kpc, has a e^{-1} width of 2 kpc, and a scale height of 100 pc. In terms of C_n^2, the inner Galaxy component is about 2000 times stronger than the outer component.

The model approximates SM data in other directions (e.g. toward the galactic poles and toward the galactic anti-center) with relatively little scatter. The large amount of scatter in Figure 4 is due to the small scale height (100 pc) of the inner Galaxy component, corresponding to a galactic latitude of only 0.7° at 8.5 kpc distance. The

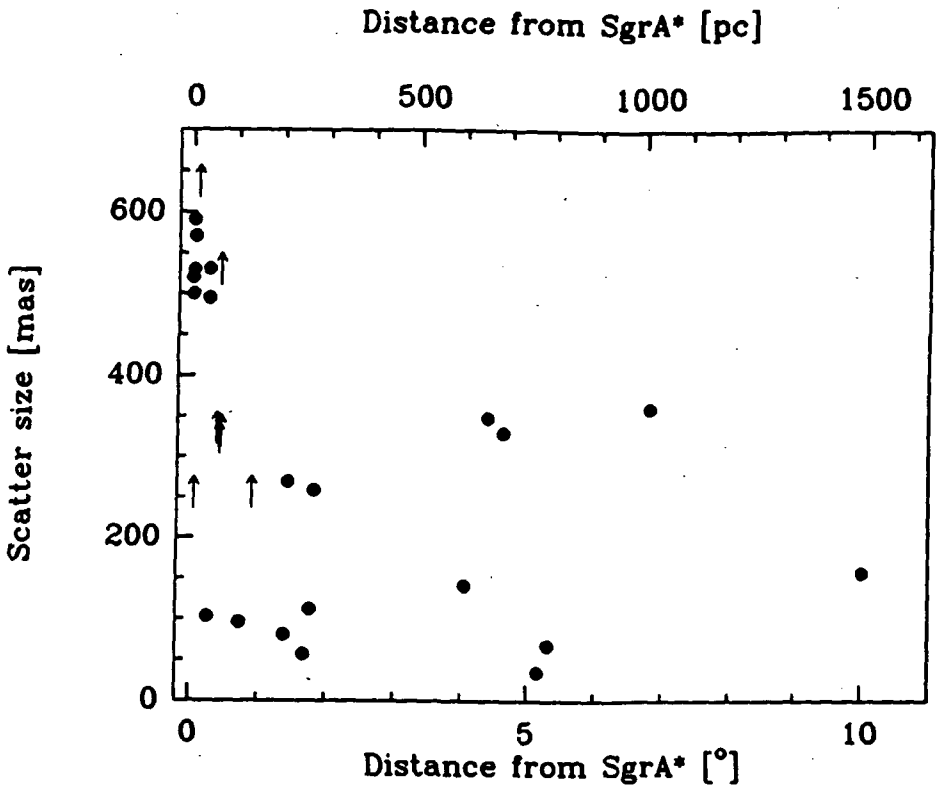

Figure 3. Plot of scatter sizes with distance from SgrA*

dotted line shows the model's SM for $|\ell| = 15°, b = 0°$ while the dashed line shows the model looking out of the galactic plane at $|b| = 5°$. Thus, points *below* the solid line may be understood as showing smaller SM because of the latitude dependence built into the model, while points *above* the line correspond to lines of sight with enhanced scattering (i.e. scattering in excess of that predicted by the model). For example, the masers inside NGC6334 show enhanced scattering (as indicated) and the AGN behind it also shows enhanced scattering. The difference in SM for the background AGN and the maser is caused by the same leverage effect presented in equations (4) and (5).

The most important feature of Figure 4 for the discussion here is the obvious enhancement of points for the sources with attributed distances of 8.5 kpc. The figure shows clearly that the scattering measures of the galactic center sources are anomalous with respect to other lines of sight toward the inner Galaxy. We note, however, that the appearance of Figure 4, namely the sudden rise of SM from that of the model to about $10^{2.4}$ kpc $m^{-20/3}$, does not prove that the enhanced scattering occurs at the distance of SgrA*; none of the other sources plotted in the figure is at the same longitude and latitude, so the onset of the large enhancement could in fact occur, at a distance smaller than 8.5 kpc.

The line of sight towards SgrA* and the 30 arcmin diameter region around it does show an enhanced level of scattering, even when compared to lines of sight in the immediate vicinity. Where, then, does this turbulent medium originate and what can

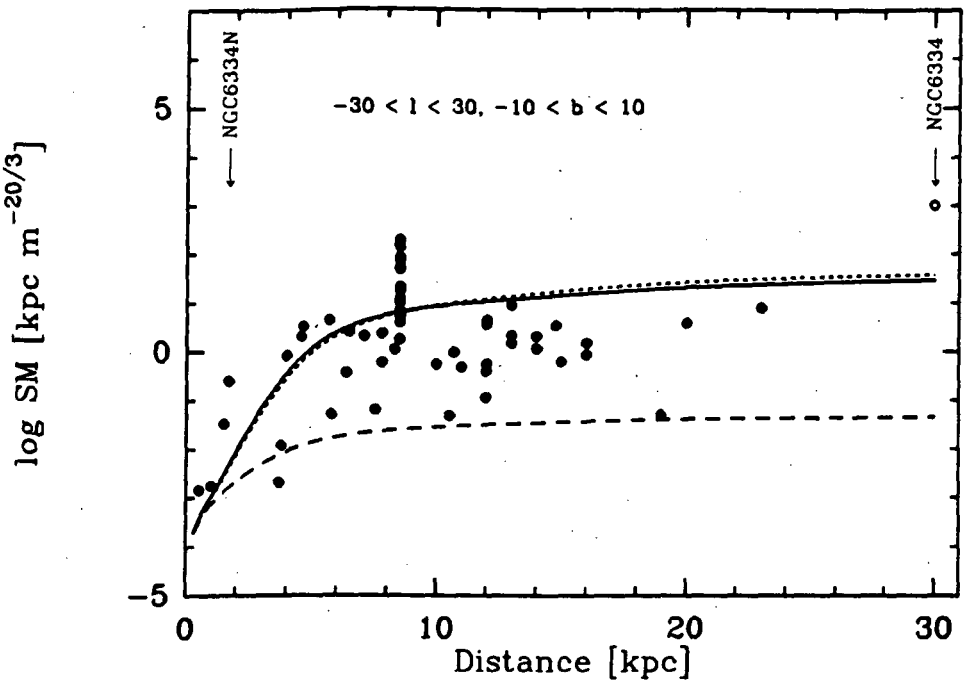

Figure 4. Plot of scattering measure against distance from the sun. The plotted points represent data presented in Tables 2 and 3 and data compiled by Cordes et al. (1991a) that include pulsar measurements and data on scattered AGNs from Fey et al. (1991). AGNs are plotted arbitrarily at a 'distance' of 30 kpc. The solid line represents SM calculated from the model of Cordes et al. for $\ell = 0, b = 0$; the dotted line corresponds to $|\ell| = 15°, b = 0$; the dashed line corresponds to $\ell = 0, |b| = 5°$.

we say about its location relative to SgrA*? We consider two possible configurations to account for the turbulence: an anomalous scattering region close to SgrA* and an unrelated turbulent region distributed in the interstellar medium towards SgrA*, but not necessarily at the same distance as SgrA*.

In the discussion we will adopt the formulas derived for very strong scattering, although the observations presented here do not yield any direct information on the presence of an inner scale. However, as pointed out in the introduction, it seems likely that observations with $\theta_{obs} > 100$ mas at 1 GHz are affected by inner scale effects. Furthermore, the observed angular size of SgrA* $\propto \lambda^2$ seems to support this conclusion.

4.2. ANOMALOUS SCATTERING LOCAL TO THE GALACTIC CENTER

Ozernoi & Shishov (1977) were the first to suggest that the scattering seen for SgrA* occurred local to the source. They calculated C_n^2 for a single scattering screen located at several different positions along the line of sight, and then, assuming an outer scale ℓ_0, they computed δn_e. They concluded that the ratio $\delta n_e/n_e$ was "reasonable" only when the scattering region was located 10 pc from SgrA*. Backer (1978) independently concluded that the scattering towards SgrA* was anomalous and gave the same distance of 10 pc for the location of the scattering screen.

Our observations also may be interpreted in terms of a local origin for the scattering. As mentioned above, the zone of enhanced scattering appears to have a well-defined angular extent of 30 arcmin, approximately centered on SgrA*, and there are no other lines of sight in our sample with comparable θ_{obs}. There are strong phenomenological reasons for believing in a local origin, as the Galactic center is arguably one of the more energetic environments in our Galaxy.

We develop a simple model to examine this hypothesis, and use it to determine the physical properties of the scattering regions. In our model we assume there is an extended medium with $C_n^2(x) = C_{n,0}^2$, and a region of enhanced scattering with $C_n^2(x) = C_{n,GC}^2$ which is distributed in a sphere centered on SgrA* with a radius R_{GC}. This model is fitted to the data and the best-fit parameters are determined using the χ^2 method. A distance of 8.5 kpc is assumed for the distance of each source. This results in a fit of $C_{n,0}^2 = 6.3\ \mathrm{m}^{-20/3}$, $C_{n,GC}^2 = 2.1 \cdot 10^8 \mathrm{m}^{-20/3}$ and $R_{GC} = 54$ pc. This value for $C_{n,GC}^2$ differs from that estimated by van Langevelde & Diamond (1991) for a similar geometry, because here we include inner scale effects.

It is tempting to try to link the enhanced scattering to a known region at the Galactic center. In this respect we note that the size of 50 pc coincides with the size of the "magnetosphere" of the Galactic center (Heyvaerts, 1989).

4.3. ANOMALOUS SCATTERING DUE TO CLUMPS AWAY FROM THE GALACTIC CENTER

It is well known that some lines of sight show enormously more scattering than neighboring ones, such as the Vela pulsar and Cygnus X-3. Moreover, the HII complex NGC6334, at $\ell = 351°$, $b = 0.7°$, and $D \approx 1.7$ kpc, causes scattering of a background extragalactic source that is larger than the scattering of the Galactic center sources discussed here (Moran et al. 1990). Cordes et al. (1985) discussed a model for the scattering medium which has a smoothly distributed component along with clumps of very strong turbulence. Clumps of parsec size were inferred to have a volume filling factor of about 10^{-4}, corresponding to a mean free path for intersection of a clump of about 5 to 10 kpc. Using a more extensive data set, a model with two smooth components has been devised (Cordes et al. 1991; as shown in Figure 4) that also must be augmented with clumps of turbulence with the same properties as the earlier model. Because the mean free path for intersecting a strong clump is less than or about equal to the distance to the Galactic center, it remains plausible that a similar clump may account for the enhanced scattering of the OH/IR masers and other sources in the Galactic center.

Previous authors have reported variations of scattering on angular scales of a few degrees or more (Fey et al. 1989, Alurkar et al. 1986, Dennison, et al. 1984). With our much finer grid of sampled points we are able to put an important limit on the typical size of a scattering clump, namely $\approx 50\ \mathrm{pc} \cdot (D/8.5\ \mathrm{kpc})$ where D is the distance of the clump from the Sun. The upper bound of 50 pc is similar to clump sizes discussed by Cordes, Weisberg, and Boriakoff (1985) and identical to that used by Fey et al. (1991) in their detailed model simulations.

4.4. IMPLICATIONS AND PREDICTIONS

4.4.1. Extragalactic sources

The model of enhanced scattering local to the Galactic center gives an interesting prediction for the observations of compact extragalactic sources, particularly those with flat spectra. Putting such a source behind the scatterer, within 15 arcminutes of SgrA*, we expect a size of 213″ *at 1.6 GHz*. For a scattering medium closer to the earth, this prediction comes out smaller, depending on the exact location of the scatterer. The best approach would be to make observations at higher frequencies (e.g. near 20 GHz with the VLA) where the angular broadening is easier to measure (if the scattering arises in the vicinity of the Galactic center). Note that angular broadening decreases faster with an increase in frequency than does the angular resolution of a telescope.

4.4.2. Physical Implications

The location of the region that causes enhanced scattering of the Galactic center sources has a large influence on the amount of free-free absorption to be expected. Consider a clump model for the variation of C_n^2 with distance from the Galactic center:

$$C_n^2(x) = \begin{cases} C_{n,0}^2 + C_{n,\mathrm{GC}}^2 & |x - L_{\mathrm{GC}}| \le \Delta L/2 \\ \\ C_{n,0}^2 & \text{otherwise} \end{cases} \tag{15}$$

where L_{gc} is the distance of the clump from the galactic center and ΔL is its thickness. Here, for simplicity, the value of C_n^2 outside the clump, $C_{n,0}^2$, is assumed to be constant and much less than that inside the clump, $C_{n,\mathrm{GC}}^2$. It may be shown, for $\Delta L/L \ll 1$, that

$$S(L) \approx \frac{1}{3} SM_0 + SM_{\mathrm{GC}} \left(\frac{L_{\mathrm{GC}}}{L}\right)^2. \tag{16}$$

The total SM is

$$SM = SM_0 + SM_{\mathrm{GC}} \approx \left(\frac{L}{L_{\mathrm{GC}}}\right)^2 S(L). \tag{17}$$

Introducing $S(L)$ from equation (17) into equation (14) and using equation (11) we obtain

$$\tau_{ff} \approx \left(\frac{L}{L_{\mathrm{GC}}}\right)^2 \left(\frac{\theta_{obs}}{7831.6\,\mathrm{mas}}\right)^2 \left(\frac{\ell_1}{100\ \mathrm{km}}\right)^{1/3} \left(\frac{\ell_0}{1\ \mathrm{pc}}\right)^{-2/3} \frac{\nu_{\theta,\mathrm{GHz}}^4\, g(\nu,T)}{\nu_{\mathrm{GHz}}^2\, T_4^{1.5}} \tag{18}$$

where $\nu_{\theta,GHz}$ is the frequency at which the angular broadening measurement θ_{obs} is obtained and ν_{GHz} is the frequency at which the optical depth is evaluated; ℓ_1 is the inner scale, while ℓ_0 is the outer scale. Using $\theta_{obs} \approx 500$ mas at $\nu_\theta = 1.6$ GHz we obtain

$$\tau_{ff} \approx 0.027 \left(\frac{L}{L_{\mathrm{GC}}}\right)^2 \left(\frac{\ell_1}{100\ \mathrm{km}}\right)^{1/3} \left(\frac{\ell_0}{1\ \mathrm{pc}}\right)^{-2/3} \frac{\nu_{\mathrm{GHz}}^{-2}\, g(\nu,T)}{T_4^{1.5}}. \tag{19}$$

To have $\tau_{ff} \le 1$ at 1.6 GHz requires that

$$\frac{L_{\mathrm{GC}}}{L} \ge 0.10 \left(\frac{\ell_1}{100\ \mathrm{km}}\right)^{1/6} \left(\frac{\ell_0}{1\ \mathrm{pc}}\right)^{1/3} \left[\frac{g(\nu,T)}{T_4^{1.5}}\right]^{1/2}. \tag{20}$$

It is possible to adjust the free parameters, particularly the temperature, to reduce the coefficient in equation (20) from 0.10 to 0.01. It is also arguable that optical depth unity occurs well below 1.6 GHz, because the spectrum for Sgr A* shows no break above 1 GHz (Lo et al. 1985). However, there is no question that the optical depth is greater than unity at 327 MHz, because Sgr A* is absent in VLA images at that frequency (Anantharamaiah et al. 1991). Indeed, Pedlar et al. (1989) conclude that τ_{ff} in front of Sgr A* is > 2.5 (at 327 MHz), though it cannot be significantly larger than this value, otherwise the spectrum would turn over above 1 GHz. This would imply that

$$\frac{L_{GC}}{L} \leq 0.32 \left(\frac{\ell_1}{100\ \mathrm{km}}\right)^{1/6} \left(\frac{\ell_0}{1\ \mathrm{pc}}\right)^{1/3} \left[\frac{g(\nu,T)}{T_4^{1.5}}\right]^{1/2}. \qquad (21)$$

Therefore, observations of Sgr A* suggest that, if the scattering and absorbing material are one and the same, then (1) the outer and inner scales of the scattering medium must be nearly equal to the fiducial values of 1 pc and 100 km, respectively; and (2) that the scattering medium is situated quite far ($\geq$ 0.85 kpc) from the Galactic center.

*4.4.3. Implications for the variability of SgrA**

The observations presented here give some idea about the electron density fluctuations close to SgrA*. Even in the model in which the scattering medium is located in the vicinity of the Galactic center, we find, from the distribution of scattered sizes, that it extends to 50 pc. A scatterer local to the Galactic center is also assumed in the discussion by Zhao et al. (1988). They infer that refractive scattering can explain the variability of SgrA* if the medium is moving with a velocity >1000 km s^{-1} relative to the source. Our observations make it unlikely that the diffractive scattering described in our paper and the refractive scattering postulated by Zhao et al. (1988) are caused by the same medium, because at a distance of 50 pc from SgrA* the velocities are reasonably well known and significantly below 1000 km s^{-1}.

4.4.4. Possible associated magnetic irregularities

Though the origin of electron density variations is unknown, it is plausible that they are related to, if not caused by, turbulence in the magnetic field such that

$$\frac{\delta n_e}{n_e} = \zeta \left(\frac{\delta B}{B}\right)^n$$

with $\zeta \approx 1$ and $n = 2$ for MHD turbulence and $n = 1$ for obliquely propagating MHD waves (Cordes et al., 1990). If $\delta n_e/n_e$ is of order unity, as it seems to be for lines of sight through the Cygnus region and for other galactic plane lines of sight (e.g. Lazio et al. 1990, Clegg et al. 1991), then the energy density in magnetic field irregularities (smaller than about 1 pc) is equal to the energy density in the large scale field.

5. Conclusions

By simple detection experiments of OH masers around the Galactic center we show that lines of sight to the Galactic center are subject to severe interstellar scattering. We also show from changes in the scattering taking place on angular scales of $\approx 20'$ that the upper limit on the size of a typical scattering clump is approximately 50 pc.

We consider two alternate interpretations for the location of the enhanced turbulence. Either it arises local to the Galactic Center, and is directly related to the violent processes going on within *or* it is due to a clump of enhanced turbulence along the line of sight, and has no physical relationship to the Galactic Center. Our data can be fit to either model equally well but the former model seems to conflict with observations of free-free absorption towards SgrA, in which the same free electrons should play a role in scattering. Further observations are suggested to help resolve this controversy.

Acknowledgements

We thank the VLBA operations team for making these observations and their processing possible, especially Joan Wrobel, Craig Walker, Barry Clark and Clint Janes. Harm Habing is thanked for his continuous advice. We are indebted to Anders Winnberg and Michael Lindqvist for letting us use their catalog prior to publication. HJvL thanks the NRAO for their hospitality, and likewise DAF thanks Sterrewacht Leiden.

DAF acknowledges the financial support of the Natural Sciences and Engineering Research Council of Canada through an NSERC Postdoctoral Fellowship and the National Radio Astronomy Observatory through a Jansky Fellowship.

JMC acknowledges NASA grant NAGW-1646 for support of this research along with support from the National Astronomy and Ionosphere Center which operates Arecibo Observatory under contract with the NSF.

References

Alcock, C., Ross, R.R., 1986, *Astrophys. J.* **305**, 837

Alurkar, S.K., Slee, O.B., Bobra, A.D., 1986, *Australian J. Phys.*, **39**, 433

Anantharamaiah, K. R., Pedlar, A., Ekers, R. D., and Goss, W. M. 1991, , submitted to *Mon. Not. R. Astr. Soc.*

Armstrong, J.W., Cordes, J.M., Rickett, B.J., 1981, *Nature* **291**, 561

Backer, D.C., 1988, in *Radio wave scattering in the interstellar medium* ed. Cordes, Rickett and Backer (American institute of Physics, New York), p 111

Backer, D.C., 1978, *Astrophys. J. (Letters)* **222**, L9

Benson, J.M., Mutel, R.L., 1979, *Astrophys. J.* **233**, 119

Bowers, P.F., Reid, M.J., Johnston, K.J., Spencer, J.H., Moran, J.M., 1980 , *Astrophys. J.* **242**, 1088

Boyd, R.B., Werner, M.W., 1972, *Astrophys. J. (Letters)* **174**, L137

Burke, B.F., Moran, J.M., Barett, A.H., Rydbeck, O., Hansson, B., Rogers, A.E.E., Ball, J.A., Cudaback, D.D., 1968, *Astron. J.* **73**, S168

Clegg, A. W., Cordes, J. M., Simonetti, J. H., and Kulkarni, S. R. 1991, submitted to *Astrophys. J.*

Clifton, T. R. and Lyne, A. G. 1986, *Nature* **320**, 43

Cordes, J.M., Weisberg, J. M., Frail, D. A., Spangler, S. R., and Ryan, M. 1991, submitted to *Nature*

Cordes, J.M., Spangler, S. R., Weisberg, J.M., and Ryan, M., 1991, submitted to *Astrophys. J.*

Cordes, J.M., Clegg, A., Simonetti, J., 1990 in *Galactic and intergalactic magnetic fields, IAU No. 140* eds. Beck, Kronberg & Wielebinski (Kluwer Academic Publishers), p 55

Cordes, J.M., Wolszczan, A., Dewey, R., Blaskiewicz, M., and Stinebring, D. R. 1990, *Astrophys. J.* **349**, 245
Cordes, J.M., Weisberg, J.M., Boriakoff, V., 1985, *Astrophys. J.* **288**, 221
Cordes, J.M., Anathakrishnan, S., Dennison, B., 1984, *Nature* **309**, 689
Cordes, J.M., Lazio, T.J., 1991, *Astrophys. J.* **376**, 123
Davies, R.D., Walsh, D., Booth, R.S., 1976, *Monthly Notices Roy. Astr. Soc.* **177**, 319
Dennison, B., Thomas, M., Booth, R.S., Brown, R.L., Broderick, J.J., Condon, J.J., 1984, *Astron. Astrophys.* **135**, 199
Diamond, P.J., Martinson, A., Dennison, B., Booth, R.S., Winnberg, A., 1988, in *Radio wave scattering in the interstellar medium* ed. Cordes, Rickett and Backer (American institute of Physics, New York), p 195
Diamond, P.J., 1989, in *Very Long Baseline Interferometry, Techniques an Applications* ed. Felli and Spencer (NATO ASI series, Kluwer), p 231
Dickinson, D.F., 1987, *Astrophys. J.* **313**, 408
Fey, A.L., Spangler, S.R., Cordes, J.M., 1991, *Astrophys. J.* **372**, 132
Fey, A.L., Spangler, S.R., Mutel, R.L., 1989, *Astrophys. J.* **337**, 730
Gaylard, M.J., West, M.E., Whitelock P.A., Cohen, R.J., 1989 , *Monthly Notices Roy. Astr. Soc.* **236**, 247
Gwinn, C.R., Moran, J.M., Reid, M.J., Schnepe, M.H., 1988, *Astrophys. J.* **330**, 817
Heyvaerts, J., 1989, in *The center of the Galaxy, IAU No. 136* eds. Morris (Kluwer Academic Publishers), p 301
Ishimaru, A., 1978, *Wave Propagation and Scattering in Random Media* (New York: Academic Press)
Kemball, A., Diamond, P.J., Mantovani, F., 1988, *Monthly Notices Roy. Astr. Soc.* **234**, 713
Kent, S.R., Mutel, R.L., 1982, *Astrophys. J.* **263**, 145
Lazio, T.J., Spangler, S. R., and Cordes, J. M., 1990, *Astrophys. J.* **363**, 515
Lindqvuist, M., Winnberg, A., Habing, H.J., Matthews, H.E., 1991, *Astron. Astrophys., Suppl. Ser.*, in press
te Lintel Hekkert, P., Caswell, J.L., Habing, H.J., Haynes, R.F., Norris, R.P., 1991, *Astron. Astrophys., Suppl. Ser.*, in press
Lo, K.Y., Cohen, M.H., Readhead, A.C.S., Backer, D.C., 1981, *Astrophys. J.* **249**, 508
Lo, K.Y., Backer, D.C., Ekers, R.D., Kellermann, K.I., Reid, M., Moran, M.J., 1985, *Nature* **315**, 124
Molnar, L., Mutel, R., Reid, M., Johnston, K., 1990, submitted to *Astrophys. J.*
Moran, J.M., 1968 *Ph.D. Thesis MIT*
Moran, J.M., Papadopoulos, G.D., Burke, B.F., Lo, K.Y., Schwartz P.R., Thacker, D.L., Johnston K.J., Knowles S.H., Reiss, A.C., Shapiro, I.I., 1973, *Astrophys. J.* **185**, 535
Moran, J.M., Rodriquez, L.F., Greene, B., Backer, D.C., 1990, *Astrophys. J.* **348**, 150
Norris, R.P., Booth, R.S., Diamond, P.J., Nyman L.Å., Graham, D.A., Matveyenko, L.I., 1984, *Monthly Notices Roy. Astr. Soc.* **208**, 435
Ozernoi, L.M., Shishov, V.I., 1977, *Sov. Astron. (Lett.)* **3**, 233
Pedlar, A., Anantharamaiah, K. R., Ekers, R. D., Goss, W. M., van Gorkom, J. H., Schwarz, U. J., and Zhao, J., 1989, *Astrophys. J.* **342**, 769
Rao, A.P., Slee, O.B., 1988, *Monthly Notices Roy. Astr. Soc.* **234**, 853
Reid, M.J., Muhleman, D.O., Moran, J.M., Johnston K.J., Schwartz, P.R., 1977, *Astrophys. J.* **214**, 60
Röttgering, H.J.A., 1989, *Astron. Astrophys.* **222**, 125
Rickett, B. J., 1990, *Ann. Rev. Ast. Ap.*, **28**, 561.
Spangler, S.R., 1988, in *Radio wave scattering in the interstellar medium* ed. Cordes, Rickett and Backer (American institute of Physics, New York), p 32
Spangler, S.R., Gwinn, C.R., 1990, *Astrophys. J. (Letters)* **353**, L29
Van der Veen, W.E.C.J., Breukers, R.J.L.H., 1989, *Astron. Astrophys.* **213**, 133
Van Langevelde, H.J., Diamond, P.J., 1991, *Monthly Notices Roy. Astr. Soc.* **249**, 7p
Van Langevelde, H.J., Van der Heiden, R., Van Schooneveld, C., 1990 , *Astron. Astrophys.* **239**, 193
Wilson, W.J., Barett, A.H., 1968, *Science* **161**, 778
Zhao, J.H., Ekers, R.D., Goss, W.M., Lo, K.Y., Narayan, R., 1988, in *The center of the Galaxy, IAU No. 136* eds. Morris (Kluwer Academic Publishers), p 535
Zhao, J.H., Frail, D.A., Roberts, D., Goss, W.M., Subrahmanyan, R., Ekers, R.D., Lo, K.Y., 1991, *in preparation*

LOW FREQUENCY ASTROPHYSICS FROM SPACE
Proceedings, Crystal City, Virginia 1990

Namir E. Kassim and Kurt W. Weiler (Eds.)

LOW FREQUENCY INTERSTELLAR SCATTERING AND PULSAR OBSERVATIONS

James M. Cordes
Astronomy Department, Cornell University

Radio astronomy at frequencies from 2 to 30 MHz challenges time tested methods for extracting usable information from observations. One fundamental reason for this is that propagation effects due to the magnetoionic ionosphere, interplanetary medium, and interstellar medium (ISM) increase strongly with wavelength. In this paper I address the problems associated with interstellar scattering off of small scale ($\sim 10^9$ cm) irregularities in the electron density.

I will first summarize what we know of interstellar scattering on the basis of high frequency observations, including scintillation and temporal broadening of pulsars and angular broadening of various galactic and extragalactic radio sources. Then I will address those high frequency phenomena that are important or, at least, detectable at low frequencies. The radio sky becomes much simpler at low frequencies: most pulsars will not be seen as time varying sources, intensity variations will be quenched or will occur on time scales much longer than a human lifetime, and many sources will be angularly broadened and/or absorbed into the noise. Angular broadening measurements will help delineate the galactic distribution and power spectrum of small scale electron density irregularities. Images of scattered sources can take on the form of the distribution of the scattering material in this low frequency regime. Spectral broadening may be a relevant line broadening mechanism for low frequency recombination lines.

Summary of Interstellar Scattering and Scintillation Phenomena

Interstellar scattering phenomena are rich in variety. *Diffraction* from small scale irregularities is manifest as angular broadening (interstellar 'seeing'); temporal broadening of pulsar pulses due to multipath propagation; and diffractive intensity scintillations. The latter have been seen only from pulsars owing to their small size (the 'stars twinkle, planets do not' rule: the critical angular size for interstellar scintillation is typically less than 1 *micro* arc sec.) Another effect, as yet unobserved from the ISM, is spectral broadening, the smearing of a spectral line due to modulations imposed by the diffracting medium. *Refraction* effects from larger irregularities include long term scintillations; wandering of apparent source positions on the sky (angle of arrival [AOA] variations); and time of arrival variations associated with the AOA variations and also with the changing electron column density (the dispersion measure, DM) as turbulence is swept across the line of sight. Figure 1 shows examples of several of these phenomena, including the visibility function of a scattered pulsar; temporal broadening of a pulsar pulse; diffractive intensity scintillations; and dispersion measure variations.

There is substantial evidence that the electron density variations responsible for the phenomena span a large range of length scale and that they may be described by a

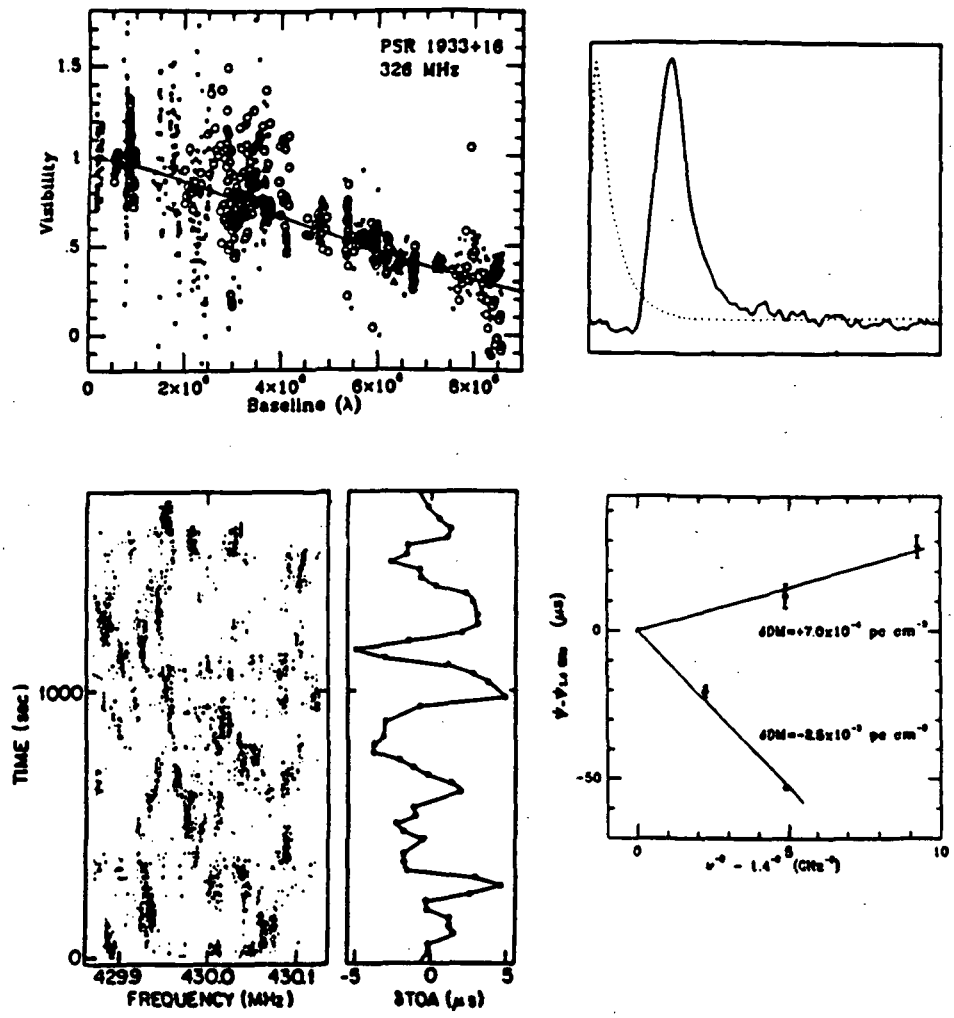

Figure 1. Examples of scattering observables: (a) visibility function[1]; (b) pulsar pulse with scattering broadening tail[2]; (c) grey scale plot of diffractive intensity scintillations[3]; (d) dispersion measure variations[4].

spatial power spectrum that is power law in form. Thus we define the power spectrum in terms of the mean square electron density:

$$\langle \delta n_e^2 \rangle \equiv \int_{q_0}^{q_1} d^3q \, C_n^2 \, q^{-\alpha}, \tag{1}$$

where we introduce the coefficient C_n^2, wavenumber cutoffs $q_{1,2}$, and spectral index α. Pulsar scintillations and time of arrival variations, and limits on AOA variations of OH masers[5] imply that $3.5 \leq \alpha \leq 4.0$. The Kolmogorov value, $\alpha = 11/3$, is consistent with many lines of sight. Defining, respectively, the 'inner' and 'outer' length scales $\ell_1 = 2\pi/q_1$ and $\ell_0 = 2\pi/q_0$ of the spectrum, limits from several kinds of observations suggest that $\ell_1 \leq 10^9$ cm and $\ell_0 \geq 10^{14}$ cm. Recent work[5,6,7] suggests that the inner scale is of the order of 100 km for a few heavily scattered lines of sight, a length scale consistent with the gyro radius of thermal ions in the warm (10^4 K) phase of the ISM. There are indirect arguments that the outer scale extends to parsec scales, based on studies of rotation measure variations[8] and on the notion that cosmic ray diffusion

requires magnetic irregularities on all scales from about 1 AU to 1 pc and that these are accompanied by density irregularities[9].

The easiest quantity to estimate, given the spectral index α, which we now assume to be 11/3, is the line of sight integral of C_n^2, which we call the *scattering measure*. The scattering measure and estimates of it using angular scattering diameters of extragalactic sources θ_{FWHM} and pulsar temporal broadening times τ_d are:

$$SM \equiv \int_0^D ds\, C_n^2(s) = \left(\frac{\theta_{FWHM}}{\theta_0}\right)^{5/3} \nu^{11/3} = A_\tau \left(\frac{\tau_d}{D}\right)^{5/6} \nu^{11/3},$$

where $\theta_0 = 0.13$ arc sec, $A_\tau = 387$ kpc $\mathrm{m}^{-20/3}$ for τ_d in seconds and D in kpc, and ν in GHz. Measured values of SM range from 10^{-4} to 10^3 kpc $\mathrm{m}^{-20/3}$. For scintillation bandwidth measurements, SM may be estimated by first using the 'uncertainty' relationship $2\pi\Delta\nu_d\tau_d = 1$ to estimate the effective temporal broadening time. For a pulsar embedded in a homogenously turbulent medium, we have

$$\theta_{FWHM} = \left[\frac{16(\ell n 2)c\tau_d}{\pi D}\right]^{1/2}.$$

In terms of the scattering diameter, the diffraction scale is $\ell_d = 2\sqrt{\ell n 2}\lambda/\pi\theta_{FWHM}$.

Spectral broadening is approximately equal to the reciprocal of the intensity scintillation time; both are due to modulations of the signal due to motion of diffracting material across the line of sight. In terms of SM, the broadening is[10]

$$\Delta\nu_s \approx \frac{V_\perp}{\ell_d} \approx 2\pi V_\perp [4\pi r_e^2 \lambda^2 C_n^2 D]^{3/5} = 1.16 \text{ Hz } V_{100}\nu^{-6/5} SM^{3/5},$$

where r_e is the classical electron radius, $V_\perp$ is the relevant transverse speed (a combination of pulsar, ISM, and Earth velocities), V_{100} is in units of 100 km s^{-1}, and SM has units of *kpc* $m^{-20/3}$, and ν is in GHz.

For galactic objects with known distances, we obtain the line of sight average $\overline{C_n^2} \equiv SM/D$. The remarkable fact is that $\overline{C_n^2}$ varies by a factor of at least 10^4 between different lines of sight. A homogenously turbulent medium would, of course, yield a constant value for this quantity. Figure 2 shows SM plotted against galactic latitude and longitude on an equal area projection. The plotted circles have diameters that are proportional to $\log SM$. It is obvious that scattering is a galactic phenomenon, since the largest circles are on lines of sight in the galactic plane. Study of how SM varies (work in progress) implies that the variation in $\overline{C_n^2}$ is due to both large scale galactic structure and localized regions of intense turbulence, including HII regions and supernova remnants. Enhanced scattering seems to be correlated over small angular scales, implying that the depth is of order a few parsecs or less. This implies that the internal C_n^2 of enhanced regions is correspondingly larger than $\overline{C_n^2}$ by a factor of about 1000.

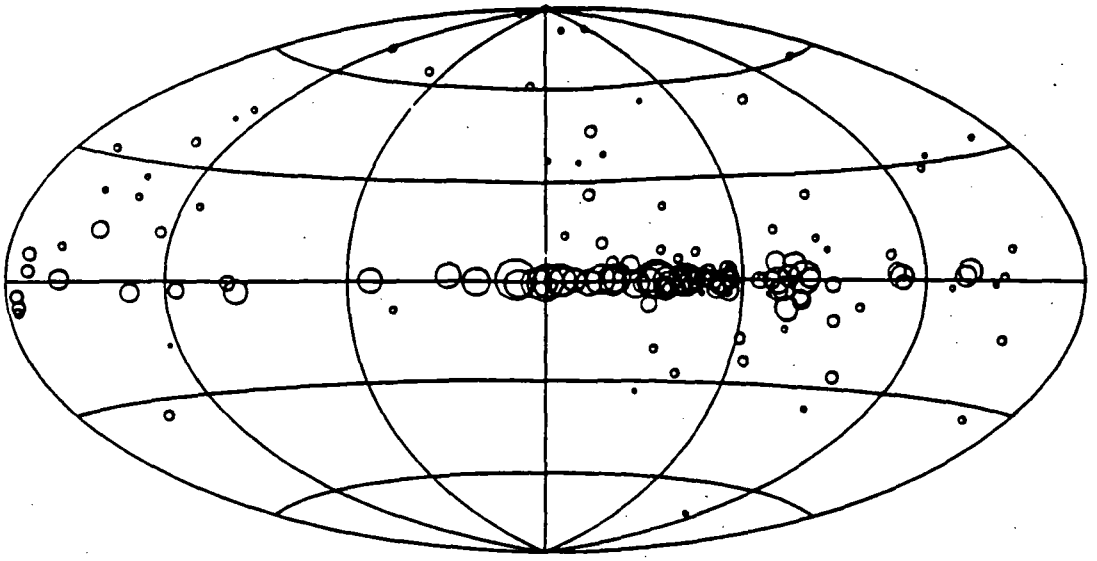

Figure 2. Scattering measures plotted versus ℓ, b; $\log SM = 3$ for the largest circles, the smallest circles have $\log SM = -4$.

To make estimates of low frequency scattering phenomena, it is useful to fit an idealized model to the data. The *local* value of C_n^2 at galactocentric radius R and distance z from the galactic plane comprises two components:

$$C_n^2(R,z) = C_1 \exp[-(R^2/A_1^2 + z/H_1)] + C_2 \exp[-(R^2/A_2^2 + z/H_2)].$$

A grid search to minimize the mean square difference between predicted and measured SM yields a large scale component with $A_1 \gtrsim 10$ kpc and $H_1 \approx 1$ kpc and a galactic center component with $A_2 \approx 3.0$ kpc and $H_2 \approx 0.05$ kpc. The strengths of the two components are $C_1 \approx 10^{-4}$ m$^{-20/3}$ and $C_2 \approx 5$ m$^{-20/3}$. This model accounts for the broad brush structure that determines SM, but there are substantial departures from the model's predictions. Figure 3 shows the modeled SM plotted against measured SM. Notable lines of sight that deviate from the model by more than two orders of magnitude include the Vela pulsar[11]; Cygnus X-3 (ref 6); and the extragalactic source behind the HII complex NGC6334B (ref 5). The grid search was iterated several times so that 'deviant' sources could be recognized and excluded from the fit. The numbers quoted above derive from the end result of this process. In a later section, the model is used to predict observable quantities such as angular broadening, spectral broadening, and temporal broadening.

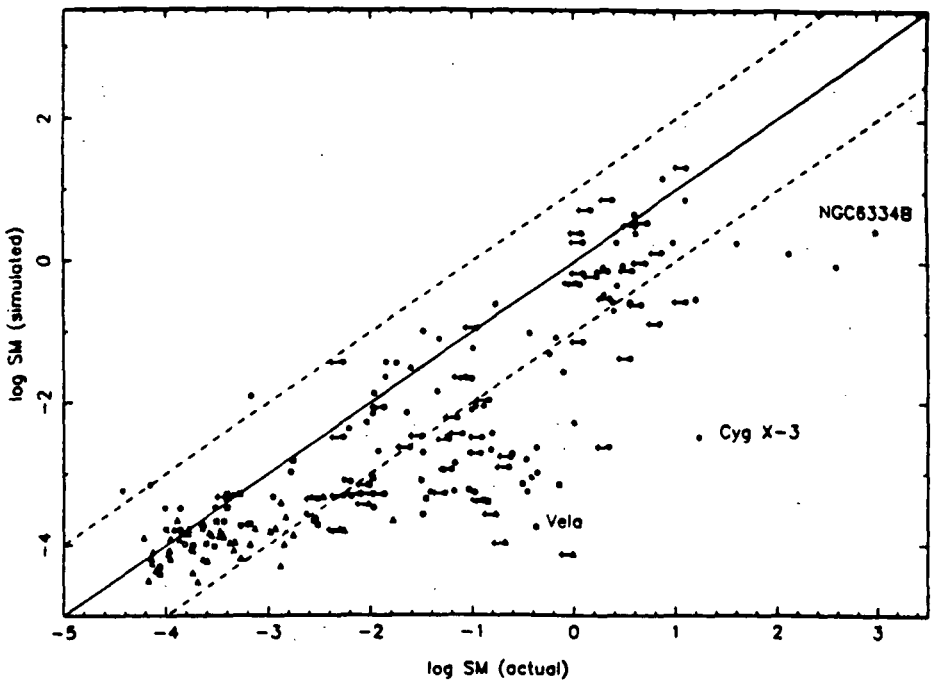

Figure 3. Modeled SM plotted against actual SM. A few notable lines of sight are labeled.

TABLE 1
DIFFRACTION PHENOMENA

Phenomenon	Quantity	Typical Values		
		400 MHz	30 MHz	10 MHz
Intensity Scintillations	$\Delta\nu \propto \lambda^{-4.4}$	10 kHz	10^{-2}	10^{-7}
	$\Delta t_d \propto \lambda^{-1.2}$	60 sec	3	0.7
Temporal broadening	$\tau_d \propto \lambda^{4.4}$	1 ms	1 min	3 hr
Angular broadening	$\theta_d \propto \lambda^{2.2}$	10 $m.a.s.$	3″	33″
Spectral broadening	$\Delta\nu_s \propto \lambda^{1.2}$	1 Hz	22	83

TABLE 2
REFRACTION PHENOMENA

Phenomenon	Quantity	Typical Values		
		400 MHz	30 MHz	10 MHz
Slow scintillations	$\sigma_I/I \propto \lambda^{-1.1}$	20%	1	0.3
	$\Delta t_r \propto \lambda^{2.2}$	1 yr	300	3000
Time-of-arrival variations	$\Delta t_{DM} \propto \lambda^2$	10μs	2 ms	16 ms
	$\Delta t_\theta \propto \lambda^{1.6}$	1μs	60	400
	$\Delta t_{\theta^2} \propto \lambda^{3.3}$	1μs	5 ms	200 ms
Angular wandering	$\Delta\theta_r \propto \lambda^{1.6}$	1 $m.a.s.$	60	400

Interstellar Scattering at Low Frequencies

Using results from high frequency observations and our understanding of the scattering medium's spectrum and distribution, it is possible to discuss the phenomena at low frequencies. In Table 1 the scaling laws[12] for various diffraction phenomena are presented and representative values of the observables are given. Intensity scintillations, which have typical frequency and time scales of 10 kHz and 60 sec at meter wavelengths become sub-Hz and subsecond at 10 MHz. In order to detect intensity scintillations, a radiometer must have sufficient signal to noise ratio for the frequency and time resolution necessary to resolve the scintillations in both time and frequency. At low frequencies where system temperatures are determined by the sky background, it is clear that diffractive scintillations will never be detectable, even for the nearest pulsar, which has the largest scintillation bandwidth. Temporal broadening becomes much larger than the pulse period of almost all pulsars at 10 MHz, so pulsars will be seen as steady sources. Angular broadening becomes a few to many arc seconds. Spectral broadening may be important for recombination line observations.

Figure 4 details the observed scattering broadening times of pulsars, showing τ_d plotted against DM . Data are taken from the literature and have been scaled to 1 GHz assuming the Kolmogorov scaling $\tau_d \propto \lambda^{22/5}$. To assess the level of temporal broadening at low frequencies, horizontal lines have been drawn (again using the Kolmogorov scaling) to show 1 sec of broadening at 10 and 30 MHz. The meaning of these lines is that all pulsars above each horizontal line will be essentially smeared out, since the average pulsar period is ~ 0.7 sec. At 10 MHz, there are only 2 pulsars below the line, while at

30 MHz, a few tens of objects are below the line. At 2 MHz, all pulsars are well above the 1 sec line (not shown). It is amusing to consider the most broadened pulsar (PSR 1849+00; ref 13) which has 1 sec of broadening even at 1 GHz. The formal scaling to 1 MHz, yields a broadening of 0.5 Myr! Note, however, that the scaling law $\tau_d \propto \lambda^{22/5}$ is based on a small angle approximation[14], which breaks down for heavily scattered lines of sight at low frequencies. Relaxing the small angle approximation gives a more reasonable result: only about 20 kyr! This means that the distribution of paths along which radiation propagates subtends a major fraction of the galactic disk. Of course, this is an academic exercise, since no source will be observable along such heavily scattered lines of sight due to free free absorption (see below).

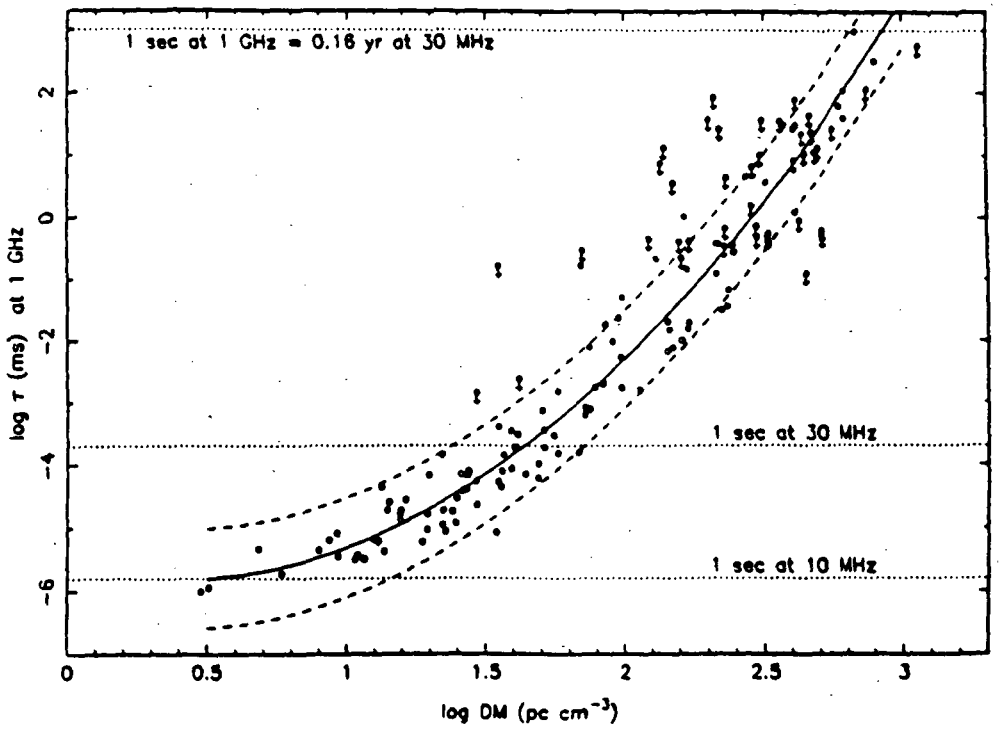

Figure 4. Pulsar temporal broadening times plotted against dispersion measure, DM. The solid line is a least squares fit to the data; the dashed lines are $\pm 1\sigma$ deviations from the fit. Downward arrows denote upper limits, which were excluded from the fit.

Refraction phenomena are presented in Table 2. Refractive scintillations occur on time scales measured in hundreds of years, so even the most dedicated of monitorers will be thwarted in variability studies. Angle of arrival variations and the associated time of arrival variations scale more slowly with wavelength than do angular and temporal broadening. As a consequence, these variations will be proportionally smaller than the angular size or pulse width and thus extremely difficult to measure at low frequencies.

Predicted Observables at Low Frequencies

The net implications for low frequency radio astronomy are that: (1) Diffractive intensity scintillations will be quenched for realistic instrumental bandwidths and time constants. This means that the equivalent of speckle interferometry in the radio will

not be possible in imaging observations. (2) Pulsar periodicities will be quenched by temporal broadening. This statement holds for all pulsars at 2 MHz, all but a few at 10 MHz, and for most at 30 MHz. (3) The time scale of refractive phenomena is much longer than a scientific career. The radio sky indeed will appear quiesent compared to high frequencies. (4) The dominant observable will therefore be the angular broadening of all kinds of radio sources. For a few pulsars in the 10 to 30 MHz band, temporal broadening can be measured, leading to determinations of the scaling law of the temporal broadening, in turn leading to further constraints on the slope and cutoffs of the wavenumber spectrum. Also, for a few pulsars, it will be possible to test whether time of arrival variations that depend on wavelength follow the λ^2 dependence of the cold plasma dispersion law, or whether TOA variations due to AOA variations are also important. These last tests will help constrain the wavenumber spectrum for δn_e on scales much larger than 1 AU. (5) Sources viewed at low galactic latitudes will be so scattered that their shapes will take on the form of the distribution of scattering material, viz. the galactic plane. This is because the maximum traversal of a ray transverse to the propagation direction is limited by the extent of the scattering medium. This source of image asymmetry has not been addressed before and competes with asymmetries due to anisotropies of the small scale irregularities themselves and distortion of a scattered image by refraction[15,16].

Using the idealized model for $C_n^2(R,z)$ discussed above, it is possible to predict the values of the most important observables at low frequencies, namely the angular broadening diameter θ_{FWHM} and the spectral broadening $\Delta\nu_c$. Figure 5 shows the angular broadening plotted against galactic latitude for several cuts in longitude.

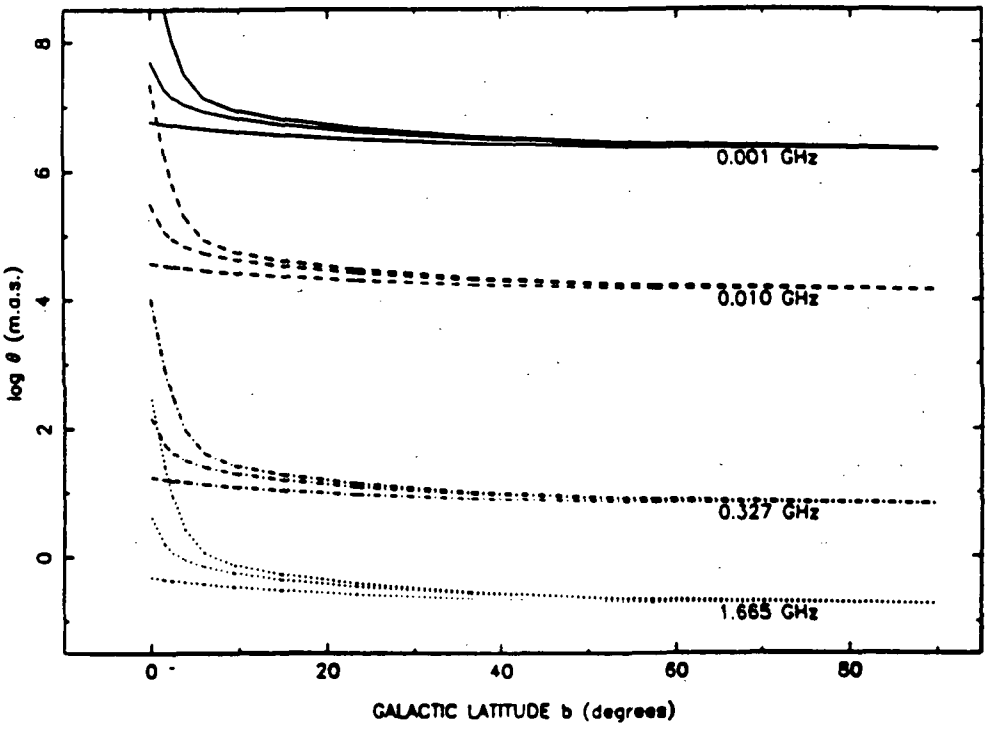

Figure 5. Predicted angular broadening of extragalactic sources vs. galactic latitude for different frequencies and for three longitudes (0, 60, and 180°.)

Spectral broadening takes on values of 300, 20, and 5 kHz at observing frequencies of 1, 10, and 30 MHz for the largest observed scattering measure (10^3 *kpc* $m^{-20/3}$ for NGC6334B, ref 5). This broadening corresponds to velocity spreads of 10^5, 500, and 50 km s^{-1}. At high latitudes, the spectral broadening is a factor of 10^4 smaller and is therefore negligible.

The spectrum defined in equation (1) implies a *lower bound* on the emission measure for a given line of sight. The total emission measure is:

$$EM = \int_0^D ds\,\langle n_e^2\rangle = \int_0^D ds\,\left[\langle n_e\rangle^2 + \langle(\delta n_e)^2\rangle\right] \equiv EM_0 + EM_\delta .$$

The line of sight integral of equation (1) gives the second term on the right hand side of the above equation. The integral of eqn (1) is

$$\langle(\delta n_e)^2\rangle = \frac{4\pi(2\pi)^{3-\alpha}}{\alpha-3} C_n^2 \ell_0^{\alpha-3}\left[1-\left(\frac{\ell_1}{\ell_0}\right)^{\alpha-3}\right] \approx \frac{4\pi}{\alpha-3} C_n^2 \left(\frac{\ell_0}{2\pi}\right)^{\alpha-1} .$$

for $\alpha \neq 3$, where the approximate equality holds for the inner scale being much smaller than the outer scale, $\ell_1 \ll \ell_0$, which seems to be a good approximation. For $\alpha = 11/3$ we have

$$EM_\delta \approx 544\,\mathrm{pc\ cm^{-6}}\ SM(\mathrm{kpc\ m^{-20/3}})\,[\ell_0(\mathrm{pc})]^{2/3} .$$

The measured values of SM therefore imply minimum emission measures of 0.05 to 10^5 pc cm^{-6} if we assume an outer scale of 1 pc. In Figure 6 we show EM_δ plotted against ℓ, b using an outer scale of 100 pc as would be measured along the lines of sight to extragalactic sources. Lines are also drawn that designate optical depth unity for several radio frequencies. It is clear that much of the Galaxy is opaque at these low frequencies. It is of interest to compare the predicted minimum EM with measured values of Reynolds[17]. For $|b| = 90°$, Reynolds obtains $EM \approx 4$ pc cm^{-6} while the scattering measurements suggest $EM_\delta(|b| = 90°) \approx 0.11\ell_0^{2/3}$. If we assume that $EM_0 \approx EM_\delta$, then an outer scale of $\ell_0 \approx 100$ pc is implied. Such an outer scale is consistent with other conjectures about the overall extent in wavenumber of the electron density spectrum[18,19].

References

1. Gwinn, C.R., Cordes, J.M., Bartel, N., and Wolszczan, A. 1988, *Ap. J. (Letters)*, **334**, L13.

2. Cordes, J.M., Weisberg, and Boriakoff, V. 1985; *Ap. J.*, **288**, 221.

3. Cordes, J.M., Wolszczan, A., Dewey, R. J., Blaskiewicz, M., and Stinebring, D. R. 1990; *Ap. J.*, **349**, 245. See also Rawley, L.A., Taylor, J. H., and Davis, M.M. 1988, *Ap. J.*, **326**, 947.

4. Gwinn, C.R., Moran, J. M., Reid, M. J., Schneps, M. H. 1988, *Ap. J.*, **330**, 817.

5. Moran, J.M., Rodriquez, L. F., Greene, B. and Backer, D.C. 1989, *Ap. J.*, in press.

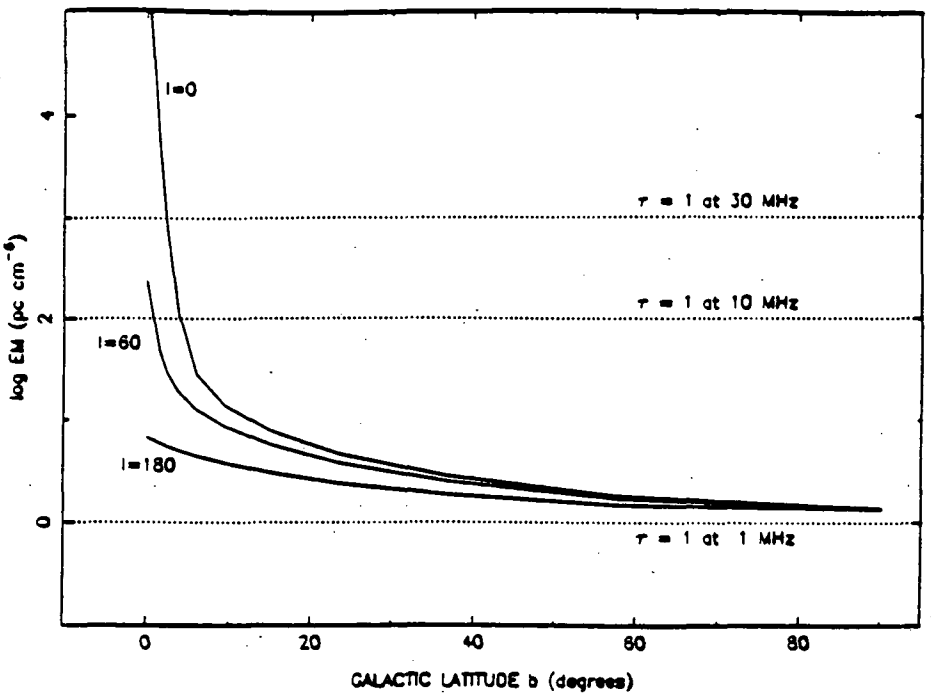

Figure 6. Predicted minimum emission measure vs. galactic coordinates.

6. Molnar, L. A., Mutel, R. L., Reid, M. J., and Johnston, K. J. 1990, *Ap. J.*, submitted.

7. Spangler, S.R. and Gwinn, C.R. 1990, *Ap. J.*, in press.

8. Simonetti, J. H., Cordes, J.M., and Spangler, S.R. 1984, *Ap. J.*, **284**, 126; Lazio, J., Spangler, S.R., and Cordes, J.M., *Ap.J.*, in press.

9. Jokipii, J. R. 1988, in AIP Proceedings 174, *Radio Wave Scattering in the Interstellar Medium*, 48.

10. Lazio, J. and Cordes, J.M., in preparation.

11. Backer, D. C. 1974; *Ap. J.*, **190**, 667.

12. Cordes, J. M., Pidwerbetsky, A., and Lovelace, R.V. 1986, *Ap. J.*, **310**, 737. See also Romani, R., Narayan, R., and Blandford, R. D. 1986, *M.N.R.A.S.*, **220**, 19; Foster, R. S. and Cordes, J. M. 1990, *Ap. J.*, submitted.

13. Clifton, T. 1985, Ph.D. Thesis, Univ. of Manchester.

14. Rickett, B. J. 1977, *Ann. Rev. Ast. Ap.*, **15**, 479.

15. Spangler, S. R. and Cordes, J. M. 1988, *Ap. J.*, **332**, 346.

16. Narayan, R. and Goodman, J. 1989, *M.N.R.A.S.*, **238**, 963.

17. Reynolds, R. J. 1990, these proceedings.

18. Armstrong, J. W., Cordes, J. M., and Rickett, B. J. 1981, *Nature*, **291**, 561.

19. Lee, L.C. and Jokipii, J. R. 1976, *Ap. J.*, **206**, 735.